REPORT DOCUMENTATION PAGE

Form Approved OMB NO. 0704-0188

1. REPORT DATE (DD-MM-YYYY)	2. REPORT TYPE	3. DATES COVERED (From - To)
18-08-2014	MS Thesis	-

4. TITLE AND SUBTITLE	5a. CONTRACT NUMBER
CHARACTERIZATION OF MWCNT/NANOCLAY BINARY NANOPARTICLES MODIFIED COMPOSITES AND FATIGUE PERFORMANCE EVALUATION OF NANOCLAY MODIFIED FIBER REINFORCED COMPOSITES	W911NF-12-1-0053
	5b. GRANT NUMBER
	5c. PROGRAM ELEMENT NUMBER
	206022

6. AUTHORS	5d. PROJECT NUMBER
Tanjheel Mahdi	
	5e. TASK NUMBER
	5f. WORK UNIT NUMBER

7. PERFORMING ORGANIZATION NAMES AND ADDRESSES	8. PERFORMING ORGANIZATION REPORT NUMBER
Tuskegee University Chemistry 1200 West Old Montgomery Rd. Tuskegee, AL 36088 -1923	

9. SPONSORING/MONITORING AGENCY NAME(S) AND ADDRESS (ES)	10. SPONSOR/MONITOR'S ACRONYM(S)
U.S. Army Research Office P.O. Box 12211 Research Triangle Park, NC 27709-2211	ARO
	11. SPONSOR/MONITOR'S REPORT NUMBER(S)
	60482-MS-REP.20

12. DISTRIBUTION AVAILIBILITY STATEMENT

Approved for public release; distribution is unlimited.

13. SUPPLEMENTARY NOTES

The views, opinions and/or findings contained in this report are those of the author(s) and should not contrued as an official Department of the Army position, policy or decision, unless so designated by other documentation.

14. ABSTRACT

Researchers have been using nanoparticles to reinforce composites for last two decades. In this research, composites were modified with binary nanoparticles consist of multi-walled carbon nanotubes (MWCNTs) and nanoclays together. First, epoxy SC-15 resin was reinforced with MWCNTs and nanoclays separately and together as binary nanoparticles and thus, nanocomposites were fabricated. To achieve uniform dispersion of nanoparticles in resin different techniques were used. MWCNTs were dispersed utilizing ultrasonication and three roll shear mixing. Nanoclay was dispersed with ultrasonication and magnetic stirring techniques, whereas, for dispersion of

15. SUBJECT TERMS

MWCNT/NANOCLAY BINARY NANOPARTICLES, DYNAMIC MECHANICAL ANALYSIS, CARBON/EPOXY COMPOSITES, FATIGUE, FLEXURE, TENSION, SCANNINF ELECTRON MICROSCOPY

16. SECURITY CLASSIFICATION OF:			17. LIMITATION OF ABSTRACT	15. NUMBER OF PAGES	19a. NAME OF RESPONSIBLE PERSON
a. REPORT	b. ABSTRACT	c. THIS PAGE	UU		Mahesh Hosur
UU	UU	UU			19b. TELEPHONE NUMBER
					334-724-4220

CHARACTERIZATION OF MWCNT/NANOCLAY BINARY NANOPARTICLES MODIFIED COMPOSITES AND FATIGUE PERFORMANCE EVALUATION OF NANOCLAY MODIFIED FIBER REINFORCED COMPOSITES

ABSTRACT

Researchers have been using nanoparticles to reinforce composites for last two decades. In this research, composites were modified with binary nanoparticles consist of multi-walled carbon nanotubes (MWCNTs) and nanoclays together. First, epoxy SC-15 resin was reinforced with MWCNTs and nanoclays separately and together as binary nanoparticles and thus, nanocomposites were fabricated. To achieve uniform dispersion of nanoparticles in resin different techniques were used. MWCNTs were dispersed utilizing ultrasonication and three roll shear mixing. Nanoclay was dispersed with ultrasonication and magnetic stirring techniques, whereas, for dispersion of binary nanoparticles all three techniques was used to achieve uniform dispersion. Nanocomposite samples were subjected to various tests to obtain mechanical, thermal and viscoelastic properties. Nanocomposites exhibited substantial improvement in almost all tests compared to the control epoxy composites. Binary nanoparticles increased flexural strength and modulus 29% and 44% respectively. Moreover, about 25% improvement in viscoelastic properties and 30% decrease in coefficient of thermal expansion were observed for binary nanoparticles reinforcement. Morphological analysis revealed that, higher resistance to crack propagation was offered by binary nanoparticles. Then, carbon fiber reinforced epoxy SC-15 composites were modified with binary nanoparticles. Carbon fiber/epoxy composites were also modified with MWCNTs and nanoclays separately to compare the properties. Carbon fiber/epoxy composites with and without nanoparticles were subjected to tensile and flexure test, dynamic mechanical analysis, thermomechanical analysis as well as morphological analysis. Binary nanoparticles modified carbon fiber/epoxy composites exhibited 30% and 31% improvement in flexural strength and modulus. Storage modulus, loss modulus and glass transition temperature increased about 40%, 44% and 19%, as well. Moreover, coefficient of thermal expansion decreased about 30% and 44% before and after glass transition temperature. Furthermore, morphological analysis ensured better adhesion between matrix and fiber for binary nanoparticles reinforced composites. Fatigue performance of nanoclay reinforced epoxy composites was evaluated in this research. Fatigue test of composites was conducted at 90%, 80% and 70% stress level of ultimate tensile strength. Nanoclays could not increase the fatigue life of composites substantially at 90% stress level, yet at 80% and 70% stress levels nanoclays reinforced carbon fiber/epoxy composites exhibited significantly higher life cycle than the control carbon fiber/epoxy composites.

THESIS APPROVED BY

_____
Major Professor

_____
Dean of College

_____
Dean of Graduate Program

For

TANJHEEL HASAN MAHDI

CHARACTERIZATION OF MWCNT/NANOCLAY BINARY NANOPARTICLES MODIFIED COMPOSITES AND FATIGUE PERFORMANCE EVALUATION OF NANOCLAY MODIFIED FIBER REINFORCED COMPOSITES

_____
Title of Thesis

CHARACTERIZATION OF MWCNT/NANOCLAY BINARY NANOPARTICLES MODIFIED COMPOSITES AND FATIGUE PERFORMANCE EVALUATION OF NANOCLAY MODIFIED FIBER REINFORCED COMPOSITES

By

TANJHEEL HASAN MAHDI

Advisor: Dr. Mahesh V. Hosur

A Thesis Submitted to the Graduate Faculty
of Tuskegee University
in Partial Fulfillment of the Requirements
for the Degree of

MASTER OF SCIENCE IN MATERIALS SCIENCE AND ENGINEERING

TUSKEGEE UNIVERSITY
Tuskegee, Alabama 36088
April 21, 2014

ACKNOWLEDGEMENTS

CONTENTS

LIST OF FIGURES

LIST OF TABLES

CHARACTERIZATION OF MWCNT/NANOCLAY BINARY NANOPARTICLES MODIFIED COMPOSITES AND FATIGUE PERFORMANCE EVALUATION OF NANOCLAY MODIFIED FIBER REINFORCED COMPOSITES

By

TANJHEEL HASAN MAHDI

ABSTRACT

Researchers have been using nanoparticles to reinforce composites for last two decades. In this research, composites were modified with binary nanoparticles consist of multi-walled carbon nanotubes (MWCNTs) and nanoclays together. First, epoxy SC-15 resin was reinforced with MWCNTs and nanoclays separately and together as binary nanoparticles and thus, nanocomposites were fabricated. To achieve uniform dispersion of nanoparticles in resin different techniques were used. MWCNTs were dispersed utilizing ultrasonication and three roll shear mixing. Nanoclay was dispersed with ultrasonication and magnetic stirring techniques, whereas, for dispersion of binary nanoparticles all three techniques was used to achieve uniform dispersion. Nanocomposite samples were subjected to various tests to obtain mechanical, thermal and viscoelastic properties. Nanocomposites exhibited substantial improvement in almost all tests compared to the control epoxy composites. Binary nanoparticles increased flexural strength and modulus 29% and 44% respectively. Moreover, about 25% improvement in viscoelastic properties and 30% decrease in coefficient of thermal expansion were observed for binary nanoparticles reinforcement. Morphological analysis revealed that, higher resistance to crack propagation was offered by binary nanoparticles. Then, carbon fiber reinforced epoxy SC-15 composites were modified with binary nanoparticles. Carbon fiber/epoxy composites were also modified with MWCNTs and

nanoclays separately to compare the properties. Carbon fiber/epoxy composites with and without nanoparticles were subjected to tensile and flexure test, dynamic mechanical analysis, thermomechanical analysis as well as morphological analysis. Binary nanoparticles modified carbon fiber/epoxy composites exhibited 30% and 31% improvement in flexural strength and modulus. Storage modulus, loss modulus and glass transition temperature increased about 40%, 44% and 19%, as well. Moreover, coefficient of thermal expansion decreased about 30% and 44% before and after glass transition temperature. Furthermore, morphological analysis ensured better adhesion between matrix and fiber for binary nanoparticles reinforced composites.

Fatigue performance of nanoclay reinforced epoxy composites was evaluated in this research. Fatigue test of composites was conducted at 90%, 80% and 70% stress level of ultimate tensile strength. Nanoclays could not increase the fatigue life of composites substantially at 90% stress level, yet at 80% and 70% stress levels nanoclays reinforced carbon fiber/epoxy composites exhibited significantly higher life cycle than the control carbon fiber/epoxy composites.

1. Chapter I INTRODUCTION

1.1 Background

Fiber reinforced polymers (FRPs) are popular alternatives to conventional metallic materials in aviation, naval and automotive industries due to their low density, higher specific strength and stiffness, higher corrosion resistance and improved fatigue performance. Primary components of FRPs are fibers and matrix where, fibers carry the load and matrix acts as a binder of load carrying fibers. In recent times, 40% of the structural components of BOEING-787 aircraft are fabricated by fiber reinforced composites. Moreover, FRPs are used extensively in submarine, sports car and sporting goods. Therefore, performance of these FRPs under various loading condition; such as axial, torsional and impact loading is very crucial for the design of structural components. Researchers have been investigating various modification of FRPs to enhance the mechanical properties, thermal stability and resistance against environmental degradation. Filler materials are incorporated with FRPs to enhance mechanical, thermal, viscoelastic properties. Filler materials are generally infused with matrix.

Thermoset and thermoplastic are two primary categories of polymers used industrially. Thermosets are rigid structures where cross-linking between polymer molecules resulting in high strength, modulus and dimensional stability. Thermoplastics are flexible structures in which there is no chemical connection between individual molecules. As a result, they possess lower strength, modulus and dimensional stability.

Fibers are the primary load carrying components of FRP composites. Fibers are considered for structural components depending on their operational environment. Among them carbon fiber is one of the most widely used fibers with exceptional specific strength and modulus, negative thermal expansion coefficient, superior thermal stability, high thermal and electrical conductivity. Mechanical properties along the fiber axis of carbon fiber are significantly higher than other fibers, whereas their through thickness and strain to failure properties are low. Therefore, in this research mechanical, thermal and viscoelastic properties of carbon fiber composites are investigated while reinforced with binary nanoparticles.

Fiber reinforced composites are renowned for their fatigue performance. Wind mill blades, automotive parts and aircraft components are frequently subjected under fatigue load. Fatigue properties of FRPs are significantly better than traditional materials. Thus, utilization of FRPs instead of conventional materials as structural components under fatigue loading is becoming popular. Therefore, in this research fatigue properties of nanoclays reinforced FRPs are analyzed and compared with the control epoxy.

1.2 Motivation

To improve the properties of both thermoset and thermoplastic composites, researchers have been using nanoparticles. The advantages of nanoparticles are their high specific strength and modulus along with low density. Moreover, addition of very low percentage of nanoparticles can enhance the properties of composites significantly. Various organic and inorganic nanoparticles are used as reinforcement of composites. Among them, carbon nanotubes (CNTs) are the strongest materials known to man. CNTs have high length to diameter aspect

ratio. Yet, CNTs are expensive and hazardous materials. Less expensive organic materials like nanoclays are also popular for composite reinforcement. Nanoclays are layered structures capable of reinforcing the matrix to enhance mechanical properties. They act as thermal and moisture barrier to provide thermal stability and environmental degradation resistance.

Recently, reinforcing composites with two nanoparticles together is becoming popular. Sometimes, two or more nanoparticles are synthesized together and applied as reinforcement to composites. Then they are called hybrid nanoparticles. Sometimes two nanoparticles are used as reinforcement despite being synthesized separately. This combination is named as binary nanoparticles. Generally, nanoparticles employed together possess different physical and chemical properties to be compatible together. Thus, in this research, CNTs and nanoclays are employed as binary reinforcement for composite reinforcement.

1.3 Approach

It is important to maximize the potential of nanoparticles in strengthening FRPs. In this research, two different nanoparticles are used to reinforce carbon fiber epoxy composites altogether and separately. The nanoparticles are COOH-functionalized MWCNTs and montmorillonite nanoclays surface modified with 25-30% octadecylamine. In previous research, 0.3 wt. % of MWCNTs reinforcement exhibited the best mechanical properties among MWCNTs reinforced carbon fiber epoxy composites. Likewise, 2 wt. % nanoclays reinforcement exhibited the best mechanical properties among nanoclays reinforced carbon fiber epoxy composites. Higher percentages of nanoparticle reinforcement resulted in

agglomeration leading to lower mechanical properties. Therefore, the approach is to find other means to obtain better properties from FRPs. Thus, utilization of binary nanoparticles to reinforce composites was devised. As, carbon nanotubes are expensive and hazardous to health, lower weight percentages of CNTs (0.1 wt. %) was combined with optimum percentages of nanoclays (2 wt. %) to form binary nanoparticles and used as reinforcement.

Dispersion of nanoparticles is always a challenge for the researchers. In this laboratory, ultra-sonication followed by three-roll shear mixing technique were used previously for dispersing nanotubes in resin. In this research, nanotubes were dispersed following the above mentioned procedure. Likewise, uniform dispersion of nanoclays was successfully achieved by sonication followed by magnetic stirring. In both cases, the nanoparticles were infused in part A of the two part resin. To achieve proper dispersion of binary nanoparticles, all the above mentioned techniques- sonication, magnetic stirring and three-roll shear mixing were used. Nanocomposites were cured at elevated temperature. In the case of fiber reinforced composites, hand layup and compression mold were used to cure at elevated temperature and pressure. Both nanocomposites and fiber reinforced composites were cut into samples of a specific size according to ASTM of various mechanical and thermal testing.

1.4 Objectives

Primary objectives of this research are following:

➢ To achieve proper dispersion of carbon nanotubes, nanoclays and binary nanoparticles in epoxy resin to fabricate nanocomposites and fiber reinforced composites.

➢ To investigate and compare mechanical, thermal and viscoelastic properties of nanocomposites with control epoxy samples.

➢ To investigate mechanical, thermal and viscoelastic properties of fiber reinforced composites by conducting tensile test, flexure test, dynamic mechanical analysis, thermomechanical analysis and morphological investigation. Comparison of the properties obtained from binary nanoparticles reinforced FRP samples with single nanoparticles reinforced FRP samples and control FRP samples.

➢ To evaluate and compare fatigue properties of nanoclays reinforced FRP composites with the properties of control ones.

1.5 Layout of thesis

Chapter I provides a brief discussion about structure and application of polymer nanocomposites and fiber reinforced composites. Moreover, motivation for this thesis is discussed briefly. Approach taken in this thesis is illustrated in this section along with objectives of this research work.

Chapter II provides a brief description on earlier researches conducted in this area. Structures of nanoparticles, fabrication techniques and characteristics of nanocomposites and fiber reinforced composites presented by researchers previously are discussed in this section.

Chapter III contains details on materials used in research and experimental procedures. The detailed properties of materials used in this research are enlisted in this section. Fabrication process of nanocomposites and fiber reinforced composites is also described. Last but not the

least, brief discussion about characterization techniques applied on the composites takes place in this section.

Chapter IV contains results obtained from experiments conducted on nanocomposites and discussion on obtained results. Nanocomposites were subjected to various mechanical, thermomechanical and viscoelastic tests. Detailed analysis on results was performed to compare between control and nanophazed samples. Discussion on probable reason for obtained results is described in this section.

Chapter V contains characterization of fiber reinforced composites. Carbon fiber/epoxy composites were subjected to mechanical and tensile tests, dynamic mechanical analysis and thermomechanical analysis.

Chapter V contains conclusion of this research work and recommendation on possible future works. Summary of outcome from all the tests conducted in this research is presented in this section.

2. Chapter II LITERATURE REVIEW

2.1 Introduction

Composite materials are popular from the early times of civilization mainly in the weapon industry and structural components. However, nowadays a combination of fibers having high strength and modulus and matrix having ductile behavior. These fibers carry the loads and their diameters are in micron range. To achieve targeted properties, fibers are oriented in a different direction in the composites. Recently, nanoparticles have come into the light, due to their ability to enhance the properties of composite materials. Nanoparticles are incorporated in the resin to fabricate composites as well as with resin and fiber together to fabricate laminated composites. Recently, fiber reinforced composites are widely used in aircraft, bridge, marine vehicles and wind turbines, where they are subjected to repetitive loading or fatigue loading. So, fatigue performance of composite materials is crucial. Fatigue life of composite materials is said to be infinite compared to traditional materials. Moreover, incorporating nanoparticles increase the fatigue performance of composite materials.

2.2 Nanoparticles incorporated in fiber reinforced composites

Nanoparticles are incorporated as fillers with polymers to enhance the performance of the composites. Nanocomposites are nanoparticle reinforced resin systems. Various nanoparticles are used to reinforce polymers. Alexandre et al. categorized layered silicate as Hectorite, Saponite, Montmorillonite, Synthetic mica. They concluded that less than 5% of these nanoparticles reinforcement results in enhancement of thermo-mechanical properties while used as reinforcement of various thermoplastic polymers (Alexandre & Dubois, 2000).

Likewise, thermoset polymers are extensively reinforced with nanoparticles. Zhou et al. incorporated various weight percentage of carbon nanofibers to epoxy and found that 2 wt. % reinforcement resulted in best tensile strength and modulus (Zhou, Akanda, Jeelani, & Lacy, 2007). Hollow particles filled composites also known as sandwich structures reinforced with 0.25 wt. % carbon nanofibers exhibited better mechanical properties compared to control foam composites not containing any nanofibers (Dimchev, Caeti, & Gupta, 2010). In addition to two-phase composites, nanoparticles are used along with short and long micron-sized fibers as multi-scale reinforcement. Multiscale reinforcement with layered silicate and glass fiber of thermoplastic polymers shows significant improvement in mechanical properties at higher temperature (Vlasveld, Daud, Bersee, & Picken, 2007). Various types of carbon nanofibers reinforced nanophazed fiber/epoxy composite exhibits higher mechanical, thermomechanical and viscoelastic properties than control fiber/epoxy composites (Chen et al., 2013; Green, Dean, Vaidya, & Nyairo, 2009; Zhou, Pervin, Jeelani, & Mallick, 2008). Halloysite nanotubes reinforced carbon fiber/epoxy composites enhance viscoelastic properties of composites (Ye, Chen, Wu, & Chan, 2011). Among these nanoparticles, carbon nanotubes and nanoclays are most widely used ones. Therefore in this research, both carbon nanotubes and nanoclays are used as binary nanoparticles.

2.2.1   Carbon Nanotube

Carbon nanotubes (CNTs) are called as strongest materials on earth. Both experimental and modelling on carbon nanotubes revealed the strength of CNTs is 50-200 GPa and stiffness of CNTs is higher than 1 TPa (Qian, Wagner, Liu, Yu, & Ruoff, 2002; Thostenson, Ren, &

Chou, 2001). Along with superior strength and modulus, exceptionally low density and high structural perfection earned carbon nanotubes highest potential as reinforcement of polymers.

Nanotubes were first synthesized in 1991 by Iijima (Iijima, 1991). Nanotubes are cylindrical structures of rolled graphitic sheets with end caps of half-fullerene structures. Primarily, carbon nanotubes can be divided into single-walled carbon nanotubes (SWCNTs) and multi-walled carbon nanotubes (MWCNTs). SWCNTs consist of a single roll of graphite sheet with a diameter of 1.4 nm whereas MWCNTs are comprised of layers of graphite sheets with diameter of 2-25nm.
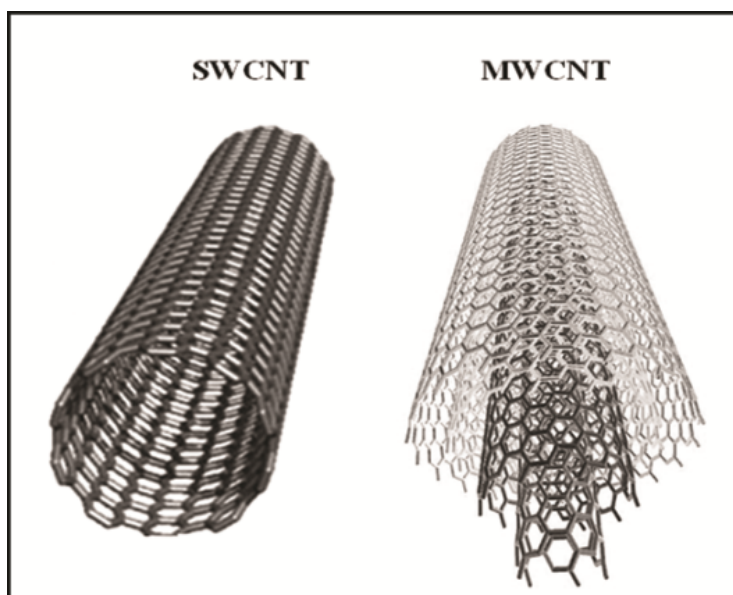
Figure 2.1 Structure of SWCNT and MWCNT (Choudhary & Gupta, 2011)

Compressive loading on CNTs revealed 60% higher young's modulus for SWCNTs than MWCNTs. When dispersed in the resin, SWCNTs exhibit more than 1 TPa modulus whereas MWCNTs show modulus about 1TPa (Cooper, Young, & Halsall, 2001). Advantages of MWCNTs over SWCNTs are feasibility of mass production, much lower production cost,

and higher thermal stability and chemical resistance (Choi, Zhang, Science, & Llc, 2014). Structures of MWCNTs and SWCNTs are depicted in figure 2.1 (Choudhary & Gupta, 2011). All these properties have led researchers to devise CNT as reinforcement to polymer composites. Rheological and dynamic mechanical properties of CNTs reinforced thermoplastic composites exhibit better dynamic mechanical properties maintaining ease of processing (Teng et al., 2008). Carbon nanotube reinforced epoxy polysulfide nanocomposites exhibit about 60% increase in tensile strength and modulus (Shirkavand Hadavand, Mahdavi Javid, & Gharagozlou, 2013). Park et al. reinforced epoxy with long-MWCNTs and entangled-MWCNTs and observed long-MWCNT to be more efficient in enhancement of thermal properties (Park et al., 2012). Both rubbery and glassy epoxy resins were experimented incorporating with CNTs. They obtained 28% enhancement in tensile modulus and 50% in impact toughness for rubbery and glassy epoxy resins respectively (Liu & Wagner, 2005). Multi-scale reinforcement along with micron-sized fiber is also popular for CNTs. CNTs and short carbon fibers synergistically enhance the mechanical properties of epoxy composites (Rahmanian, Suraya, Shazed, Zahari, & Zainudin, 2014). SWCNTs modification of peek/glass fiber composites improved thermal, electrical and mechanical properties of composites (Díez-Pascual et al., 2011). Yet, to achieve desired properties from nanocomposites, proper dispersion and superior adhesion between CNTs and polymers should be ensured.

Adhesion between CNTs and polymers can be achieved by chemical bonding among them. Functionalization of CNTs plays an important role to make the nanoparticles compatible to react with polymers. Sahoo et al. discussed various method of functionalization of CNTs and

fabrication process of CNT nanocomposites (Sahoo, Rana, Cho, Li, & Chan, 2010). Addition of carboxyl functionalized MWCNTs can successfully initiate curing at lower temperature and reduce activation temperature (Jahan, Narteh, Hosur, Rahman, & Jeelani, 2013). Moreover, crosslink density was reported to be increased due to MWCNT reinforcement, although the highest crosslink density was obtained for different percentage of loading ranging from 0.3%-0.5% (M. M. Rahman et al., 2013; Srikanth, Kumar, Kumar, Ghosal, & Subrahmanyam, 2012). Electrical property enhancement was reported by Guadagno et al. due to the significant increase in electrical conductivity of MWCNTs reinforced epoxy composites (Guadagno et al., 2011). Mechanical and thermal properties of glass fiber/epoxy composites were influenced highly by amine functionalized MWCNTs (M. M. Rahman et al., 2012). Furthermore, silane surface treatment of MWCNTs results in higher tensile and fracture characteristics (Lee, Rhee, & Lee, 2010). Salam et al. compared amine and carboxyl functionalized MWCNTs and obtained better mechanical and thermal properties for carboxyl functionalized MWCNTs (Salam, Hosur, Zainuddin, & Jeelani, 2013).

Dispersion method is crucial for achieving good dispersion. Dispersion of nanoparticles in resin stands for de-agglomeration of nanoparticles and uniform distribution of nanoparticles all over the resin structure. Sonication, three roll shear mixture, magnetic stirring, mechanical stirring are commonly used dispersion techniques. Montazeri et al. applied sonication technique to achieve uniform dispersion and obtained high mechanical and thermal properties for different dispersion time and sonication energy (Montazeri & Chitsazzadeh, 2014). Yang et al. achieved uniform dispersion by TETA (triethylene-tetramine) functionalization of MWCNTs (Yang, Gu, Guo, Pan, & Mu, 2009). Combination of ultra-

sonication and three-roll shear mixing lead to better dispersion followed by better mechanical and thermal properties (M. M. Rahman et al., 2012; M. Rahman et al., 2013). Zainuddin et al. reported combined dispersion method with and without acetone media and concluded that, dispersion in acetone media resulted in about 72% improvement of viscoelastic properties (Zainuddin et al., 2014). Diversified application and high prospect of carbon nanotubes come at a great price; CNTs are hazardous to animal and plant life (Du, Wang, You, & Zhao, 2013). This hazardous effect of CNTs leads researchers to use organic nanoparticles like nanoclays.

2.2.2 Nanoclays

Clay particles are plate like structures with a thickness only up to 3nm while in lateral directions ranging from 200 to 600 nm. Clay particles primarily consist of sheets of tetrahedral silicon-oxygen structure and octahedral Aluminum- oxygen or hydroxyl structure. According to the number of layers, clay particles are two types: (1:1) Kaolinite group, containing one tetrahedral sheet bonded by hydrogen bonds with one octahedral sheet and (2:1) silicate group comprised of two tetrahedral sheet bonded with the opposite sides of an octahedral sheet by hydrogen bond and van der-walls force between the layers depicted in figure 2.2 (Hegde, 2009). According to the distance between layers, silicates are divided into illite, smectite, vermiculite, and chlorite. Smectite group is subdivided into nontronite, hectorite, saponite and montmorillonite (MMT). Among these layered silicates, MMT is most widely used to fabricate nanocomposites as reinforcement due to its abundance in nature at low cost and is environment friendly.
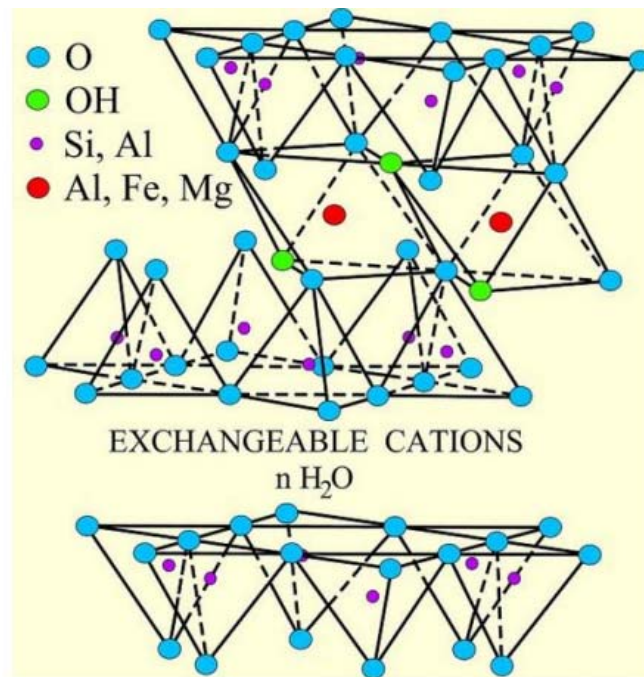
Figure 2.2 Common structure of clay particles (Hegde, 2009)

Okada et al. declared polymer-clay structures are real nanocomposites and investigated effective fabrication process for clay reinforced nylon 6 and nitrile rubber nanocomposites (Okada & Usuki, 1995). Morphology: mechanical and thermal properties of nanocomposites are highly dependent on processing technique, modification of clay and resin curing agents (Azeez, Rhee, Park, & Hui, 2013). Hegde analyzed the fabrication process and mechanical and morphological properties of nylon-6 and polypropylene nanocomposites and reported that beyond 2 wt. % loading of nanoparticles, no significant influence on properties was observed (Hegde, 2009). Thermal and mechanical behavior of clay-epoxy composites are investigated by numerous researchers and they obtained best mechanical properties for 2 wt. % of nanoclay reinforcement (Chowdhury, Hosur, & Jeelani, 2006; Xu & Hoa, 2008; Zainuddin et al., 2010; Zhou, Pervin, Rangari, & Jeelani, 2007). Although, Yasmin et al.

reported enhancement of mechanical properties up to 10% due to reinforcement of nanoclay, they reported lower thermal properties for nanoclay addition (Yasmin, Luo, Abot, & Daniel, 2006). Jumahat et al. published that, nanoclay incorporation lead to lower compressive strength for 1-5% loading of nanoclay due to non-uniform dispersion (Jumahat, Soutis, Mahmud, & Ahmad, 2012). Micro-hardness properties of nanoclay/epoxy composites were experimented by Lam et al. and 4 wt. % loading resulted in better hardness (C.-K. Lam et al., 2005). Moreover, nanoclay acts as toughening agent while incorporated with epoxy system by only 1 wt. % (Sancaktar & Kuznicki, 2011). Therefore, 3-5 wt. % nanoclays reinforcement with FRPs resulted in higher impact properties (Avila, Soares, & Silva Neto, 2007; Iqbal, Khan, Munir, & Kim, 2009). Tcherbi-Narteh et al. investigated influence of various nanoparticles on viscoelastic properties of nanocomposites and reported best properties for Cloisite 30B incorporation (Tcherbi-Narteh, Hosur, Triggs, & Jeelani, 2013). Along with mechanical and thermal properties, nanoclay composites have superior resistance against environmental degradation, moisture absorption and corrosion. Agar/Cloisite nanoclays nanocomposites exhibit high anti-microbial function (Hong, Lee, & Rhim, n.d.). While immersed in water, addition of 5 wt. % nanoclay reduced water intake in composites up to 34% (Alamri & Low, 2013). Even, moisture absorption of composites is significantly lowered due to 5 wt. % addition of nanoparticles (Kim, Hu, Woo, & Sham, 2005). Zainuddin et al. reported 2 wt. % of nanoclay reinforced composites exhibit higher properties compared to control epoxy after 90 days environmental conditioning (Zainuddin, Hosur, Zhou, Kumar, & Jeelani, 2009). To achieve desired properties from nanoclay reinforced composites proper exfoliation of nanoclays in resin must be ensured. Researchers have applied various

techniques to ensure exfoliation of nanoclays. Lam et al. optimized sonication time for dispersing Cloisite nanoparticles (C. Lam, Lau, Cheung, & Ling, 2005). Vacuum and spinning together were applied by Chan et al. to reinforce 1-7 wt. % nanoclays successfully (Chan, Lau, Wong, Ho, & Hui, 2011). Olivier et al. reported enhancement of barrier properties of nanoclay layer due to 1-2 hours sonication (Olivier et al., 2011). In our laboratory, magnetic stirring for 24 hours have been employed by researchers successfully (Tcherbi-Narteh et al., 2013; Zainuddin et al., 2010).

2.2.3 Binary nanoparticles

Nowadays researchers are exploring a new era of nanoparticles, the synergistic effect of nanoparticles. When two nanoparticles are grown together and used as reinforcement then the combination of nanoparticles are called hybrid nanoparticles. Sometimes two nanoparticles are used together without letting them grow together to reinforce composite system. These nanoparticles may react with polymers separately and result in better properties than single nanoparticles reinforcement. These combined nanoparticles are called binary nanoparticles. Huang et al. achieved uniform dispersion easily and self-reinforced crystalline nanocomposites with the synergistic effect of fullerene and CNTs (Huang et al., 2014). MWCNTs and SiO_2 together exhibit 15.6% improvement in tensile modulus compared to the MWCNTs reinforced ones (Jia, Liu, Huang, Hui, & Yang, 2013). Reinforcing with two different sized particles is also getting popular. Combination of aluminum oxide and nitride lead to higher thermal conductivity due to the structural arrangement of the particles. The smaller among the particles fill the gap amidst the skeleton of larger particles resulting in better conductivity (S. Choi & Kim, 2013). Synergistic effect

of EPDM rubber and SiO₂ on polypropylene gives rise to impact strength of composites (H. Yang et al., 2006). Shang observed the effect of $CaCO_3$ and OMMT together on mechanical properties of High-density polyethylene and obtained an increase in both tensile and impact properties (Shang, 1999). POE elastomer and nano-$CaCO_3$ improved impact toughness of polypropylene composites without sacrificing stiffness and tensile strength (Ma, Mai, Rong, Ruan, & Zhang, 2007). Graphene platelet and carbon nanotube enhance 35.4% and 146.9% of tensile strength and thermal conductivity respectively (S.-Y. Yang et al., 2011). Polyvinylidene fluoride (PVDF) polymer reinforced with polypyrrole (PPy) and MWCNTs exhibits synergistic effect of both fillers. PPy helps MWCNT to achieve uniform dispersion resulting in bridging of PPy particles through PVDF polymers (da Silva et al., 2013). As most widely used nanoparticles, synergistic effect of CNTs and nanoclays intrigued researchers the most.

2.2.3.1 Synergistic effect of MWCNTs and nanoclays

Researchers are conducting analysis on synergistic effect of nanoclay and nanotube on properties of polymers. Delay in degradation onset temperature was observed for binary reinforcement of polymethyl methacrylate (Orhan, Isitman, Hacaloglu, & Kaynak, 2012). Significant improvement in DMA, tensile and flexural properties were achieved by 3 phr nanoclays and 1.5 phr MWCNTs treatment of wood polymer nanocomposite (Hazarika & Maji, 2014). Synergistic effect of nanoclay and nanotube reduced peak heat release and rate of degradation as well as increased activation energy significantly in thermoset and thermoplastic composites (Hapuarachchi & Peijs, 2010; Im, Lee, In, & Lee, 2010; S. K. Lee, Bai, Im, In, & Lee, 2010). Manikandan et al. reinforced fuel cell with binary CNT-nanoclay

nanoparticles and observed higher thermal stability of Nafion membrane of fuel cells (Manikandan, Mangalaraja, Avila, Siddheswaran, & Ananthakumar, 2012). 2 wt. % binary CNT and nanoclay enhances Vicker's hardness of epoxy composites about 40% (Lu, Lau, Tam, & Liao, 2006). Ahmad et al. investigated synergistic effect of nanoclays and MWCNTs on epoxy composites. They observed most significant influence of MWCNT on impact properties whereas nanoclays affects tensile properties more (Ahmad, Ahmad, Tarawneh, & Apte, 2012). Morsy et al. reported that, 6 wt. % nanoclays and 0.02 wt. % CNTs enhanced the compression properties by 29% compared to control (Morsy, Alsayed, & Aqel, 2011). Decrease in tensile strength was reported by Ayatollahi incorporating MWCNTs and nanoclays together (Ayatollahi, 2011). Vivo et al. obtained higher electrical conductivity for binary MWCNT and nanoclay reinforced composites.

2.3 Fatigue Performance of composites

To perform axial fatigue test, cyclic load is applied at a constant frequency in purely tensile aor purely compressive or mixed mode. The minimum to maximum stress ratio can be varied and denoted by R. For purely tensile and compressive loading stress ratio, R is positive and for mixed loading, R is negative. For, composite materials, purely tensile testing is conducted mostly. Also testing for tensile, compressive and mixed loading are conducted to construct CLD diagrams. ASTM standard D3479 recommends rectangular specimen for fatigue testing, which is followed by most of the researchers (Bortz, Merino, & Martin-Gullon, 2011, 2012; Khan, Munir, Hussain, & Kim, 2010; Manjunatha, Taylor, Kinloch, & Sprenger, 2010). Often premature failure occurs while using rectangular specimen, so sometimes dog-bone shaped specimen is used for fatigue testing. After testing, fatigue fracture surface is

observed with microscopes, such as Scanning Electron Microscope (SEM), transmission electron Microscope (TEM). Boger et al. proposed electrical conductivity change at the initiation of cracks to sense damage of composites (Böger, Sumfleth, Hedemann, & Schulte, 2010). Daggumati et al. observed micro-scale damage and found initiation of crack from various front of the yarns followed by damage of load carrying weaker fibers, later strong fibers were affected as same load is being carried by less number of fibers (Daggumati et al., 2013). Later delamination of plies occurs at an angle 45 degree (Bortz et al., 2011). From the observation of micro-scale fatigue damaged surface, the surface of neat composite is much smooth, whereas the surface of nanoparticle reinforced ones is rough and full of voids, which are formed due to the debonding of nanoparticles. This debonding of nanoparticles and void formation causes dissipation of energy, increasing fracture toughness as well as overall fracture surface area (Bortz et al., 2012; Manjunatha et al., 2010). For, low cycle fatigue, nanoparticles can hinder the fatigue crack growth as mentioned above, but for the high number of cycle, multiple crack fronts are initiated and nanoparticles cannot play an important role in arresting the crack propagation. Thus, nanoparticles can enhance the fatigue strength at lower cycle (Bortz et al., 2012; Davis, Wilkerson, Zhu, & Ayewah, 2010; Zhou et al., 2008). Nanoparticles incorporation tends to increase fatigue life of composites under purely compressive loading compared to purely tensile loading, whereas under mixed loading nanoparticle incorporation seems to have no significant effect. Nanoparticles provide high matrix stiffness to prevent fiber buckling, thus contributing to better compressive load performance of nanoparticle infused composites, although traditional nanomechanical mechanisms like bridging or MWCNT pull-out seemed to be less effective in this

phenomenon (Böger et al., 2010; Bortz et al., 2011). Repetition of crack opening and closing occurs due to a change in the loading direction in case of mixed mode of loading. Also, local buckling of primary micron sized fiber and high interface density are also responsible for lower performance in case of mixed loading (Bortz et al., 2011). Khan et al. and Bortz et al. performed fatigue testing using different percentage of carbon nanoparticles and found 3% nanoclay, 1% helical ribbon carbon nanofiber to be most useful (Bortz et al., 2012; Khan et al., 2010). Also, silica nanoparticle is used (Manjunatha et al., 2010).

2.3.1   S-N diagram

S-N curve is constructed by plotting the maximum in plane strength against number of cycles in a logarithmic scale. A flatter S-N curve is found for composite materials compared to isotropic materials, which delineates less fatigue sensitivity. Flatter S-N curve could not be achieved by incorporating nanoparticles, but it tends to shift to longer lives and higher stresses (Bortz et al., 2011; Manjunatha et al., 2010). S-N curves delineated that mixed mode of loading to be most fatigue sensitive followed by purely tensile loading, whereas purely compressive loading found to be least fatigue sensitive due to nanoclay incorporation (Bortz et al., 2012). Manjunatha et al. also found the S-N curves of the nanoclay incorporated composites shifted to higher stresses and longer lives, but for the bulk epoxy composites the percentage of increment is higher than for the laminated composite (Manjunatha et al., 2010). Boger et al. found much flatter S-N curve for purely compressive loading compared to tensile and compressive-tensile mixed loading by incorporating MWCNT and fumed silica nanoparticle (Böger et al., 2010). Davis et al. incorporated 0.2, 0.3, 0.5 wt. % f-XD-CNT with carbon fiber-epoxy composite, and for purely tensile and purely compressive loading,

flatter S-N curve was achieved for higher (0.3 and 0.5) CNT percentage, whereas, mixed mode of loading showed erratic behavior at transition of low to high cycle (Davis et al., 2010). In most of the cases, power fit for fatigue model or exponential fit for fatigue model is used. However, these S-N curves are constructed from the stresses observed at fatigue lifetime 10^3-10^7 followed by extrapolation for the life span less than 10^3 cycles and more than 10^7 cycles. Power law model cannot always predict the low cycle region correctly, so a binary S-N curve using an exponential model at low cycle regime and power law model at high cycle regime was proposed and verified by Sarfaraz et al. (Sarfaraz, Vassilopoulos, & Keller, 2012). Harik et al. proposed bi-linear S-N curve to predict fatigue life (Harik, Klinger, & Bogetti, 2002).

3. CHAPTER III METHOD AND MATERIALS

3.1 Introduction

In this research SC-15 epoxy resin was reinforced with various nanoparticles and carbon fiber to fabricate nanocomposites and fiber reinforced composites. All commercially available materials are utilized in this research. Different dispersion techniques such as ultrasonication, magnetic stirring and three roll mixing or their combinations are required to achieve uniform dispersion for different nanoparticles in resin. Composites are cured at high temperature. Mechanical tests such as tensile and flexure tests are conducted on composites. Thermomechanical and viscoelastic tests are also conducted to obtain coefficient of thermal expansion, storage modulus, loss modulus and glass transition temperature.

3.2 Materials

SC-15 Epoxy, a commercially available two part resin system obtained from Applied Poleramic Inc. was used in this research. It is a toughened, low viscosity (300 cps) resin having low shrinkage properties upon curing. Part A of this two part resin is diglycidyl ether of bisphenol A (DGBEA) and part B is curing agent consists of mixture of cycloaliphatic amine and polyoxylalkyl amine; mixing ratio is A:B=10:3. Chemical structure of DGEBA is shown in figure 3.1 (Tcherbi-Narteh, Hosur, Triggs, & Jeelani, 2013). This is a room temperature curing resin having pot life of 6 hours, which can also be cured at high temperature. Carbon fiber used in this study was 8 harness satin weaved carbon fiber purchased from US composites. Areal density of the carbon fiber is 0.37 kg/m^2, tow size 3k, thickness 0.46 mm and fibers are surface treated to obtain better interfacial properties

through chemical bonding formation between fiber and matrix. Carboxyl functionalized MWCNTs having diameter of 10-20nm and length 10-30 micrometer were obtained from Nanostructured and Amorphous Materials Inc. Figure 3.2 (Choudhary & Gupta, 2011) depicts approximate chemical structure of carboxyl functionalized MWCNT, which has more reactive sites than other functionalized MWCNTs (Salam et al., 2013). Nanomer I-30E, nanoclay that is surface modified with 25-30 wt. % octadecylamine was purchased from Sigma-Aldrich. Typically, nanoclay contains less than 3% of moisture with a mineral purity of 98.5%. The mean particle size is about 8-10 microns and the average density is 200-500 kg/m^3 (Alexandre & Dubois, 2000). Montmorillonite nanoclays are 2:1 phylllosilicates having chemical composition $A_{0.3}(Al_{1.3}Mg_{0.7})[Si_4]O_{10}.(OH)_2.xH_2O$, where "A" is an exchangeable cation, such as, K+. Nanoclays are hydrophilic platelets, which are commercially available with different surface modifications to make them chemically compatible with hydrophobic resins. Structure of montmorillonite nanoclay is depicted in figure 2.2.
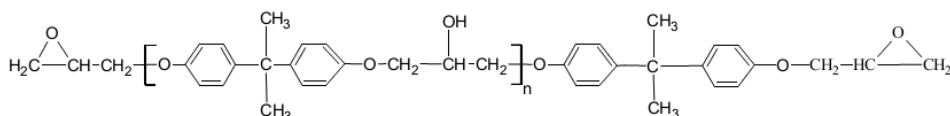
Figure 3.1 Chemical structure of DGEBA epoxy (Tcherbi-Narteh et al., 2013)
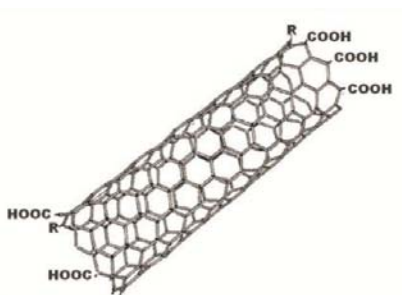
Figure 3.2 chemical structure of carboxyl functionalized MWCNTs (Salam et al., 2013)

3.3 Fabrication Process

Fabrication process included four different types of samples: Carbon fiber reinforced epoxy composites (CFRPs) serve as control laminates, MWCNT modified CFRPs, nanoclay infused CFRPs as well as 0.1 wt. % MWCNT/ 2wt. % nanoclay binary nanoparticles reinforced CFRPs. Various dispersion techniques were applied to break up the agglomeration and ensure proper dissemination of nanoparticles in the resin.

3.3.1 Dispersion of COOH-MWCNT into epoxy resin

High aspect ratio of MWCNTs leads to entanglement of nanotubes among themselves due to van der Waals forces, which is the principal reason for agglomeration of MWCNTs. Hence, insuring de-agglomeration and uniform dispersion of MWCNTs in resin is a major challenge. Functionalization of MWCNTs assists the dispersion process with the positive or negative charge of functional group, which undermines the van der Waals forces (Soliman, Sheyka, & Taha, 2012). Several methods of dispersion, such as, mechanical and magnetic stirring (Soliman et al., 2012), sonication (M. M. Rahman et al., 2012, 2013; Salam et al., 2013) and high speed shear mixing (Kostopoulos, Baltopoulos, Karapappas, Vavouliotis, & Paipetis, 2010; M. M. Rahman et al., 2012; M. Rahman et al., 2013) has been reported by researchers. In our study, desired amount of carboxyl functionalized MWCNT was weighed and mixed with calculated amount of epoxy part A manually. Then the mixture was ultrasonicated at a temperature about 40°C for 30 minutes at 39% amplitude and 30 second on /20 second off pulsating cycle to ensure uniform dispersion. Elevated temperature was used to reduce viscosity of resin as nanoparticle addition tends to increases the viscosity and dispersion

becomes difficult. To facilitate the dispersion and minimize the agglomeration, three roll mill was used as a high speed shear mixer. It consists of three rollers, where first and third rollers rotate in opposite direction of second roller to enforce high speed shearing in the resin and nanoparticle mixture. Differential speed of rotation of rollers is controlled by a gear mechanism with a ratio of 1:3:9. In our study, the maximum speed of 150 rpm was maintained while passing the mixture of resin and MWNCTs three times between the rollers. Gap between successive roller rollers was maintained same during each pass. Setting of the same was 20μm for first pass, 10μm for second pass and 5μm for the final pass. Varying speed and contra-rotation of successive rollers enhanced uniform dispersion of nanoparticles in resin.

3.3.2   Dispersion of Montmorillonite nanoclay into epoxy resin

Nanoclays are hydrophilic organoclays prone to moisture when exposed to open air. I-30E nanoclays contain about 3% moisture. To drive off the moisture and obtain entirely dry nanoclays, they are placed in vacuum at a temperature 50 °C overnight. Besides, nanoclays are layered structures, so complete exfoliation of nanoclays with epoxy resin is to be ensured as well as uniform dispersion. To ensure that, magnetic stirring (Tcherbi-Narteh et al., 2013; Zainuddin, Hosur, Zhou, Kumar, & Jeelani, 2009), high speed mechanical mixing (Alamri & Low, 2013; Iqbal, Khan, Munir, & Kim, 2009), ultrasonication (Iqbal et al., 2009) methods are preferred by researchers. In this study, sonication and magnetic stirring were used. At first, calculated amount of nanoclay was weighed and mixed with resin manually and ultrasonicated using same conditions as in the case of nanotubes. Then the mixture was

magnetically stirred at 800 rpm for 24 hours at a temperature 50 °C. Elevated temperature was used to reduce viscosity of resin to facilitate nanoclay dispersion.

3.3.3 Dispersion of binary nanoparticles into epoxy resin

In order to disperse MWCNTs and nanoclay together combination of various methods was applied and uniform dispersion was achieved through a complex and prolonged procedure based on our prior studies. In this process, MWCNTs were mixed with epoxy through ultra-sonication for 20 minutes at 39% amplitude and 30 second on/20 second off pulse cycle to ensure uniform dispersion. Then nanoclays were added and the mixture was ultrasonicated again for 15 minutes using same conditions. After that, the mixture was stirred magnetically at 800 rpm for 24 hours at a temperature 50 °C. Finally, three-roll shear mixer was used to ensure consistent and uniform dispersion of binary nanoparticles in the epoxy resin.

3.3.4 Nanocomposite fabrication

After dispersion, part A of SC-15 epoxy containing nanoparticles was mixed with part B at a ratio 10:3. High speed mechanical mixing was done for 10 minutes to obtain a stoichiometric mixture, which was then utilized as matrix for laminates. For control samples, only Part A and part B of SC-15 resin were mixed at a stoichiometric ratio and used as matrix. The resin mixture was degasified by placing it in vacuum oven for about half an hour to remove the bubbles formed in the resin due to the mechanical mixing in both cases. The resin and nanoparticles mixture was then poured in a steel mold. The molds were fabricated according to the required size for samples. The molds are pre-heated at a temperature 60 °C to avoid sudden temperature change for resin-nanoparticles mixture, which was degassified at higher

temperature to increase fluidity. Molds containing liquid resin-nanoparticles mixture are then placed in the oven at 60 °C for one hour and 120 °C for two hours to achieve full curing of the samples. Nanocomposites fabrication procedure is portrayed in figure 3.3.
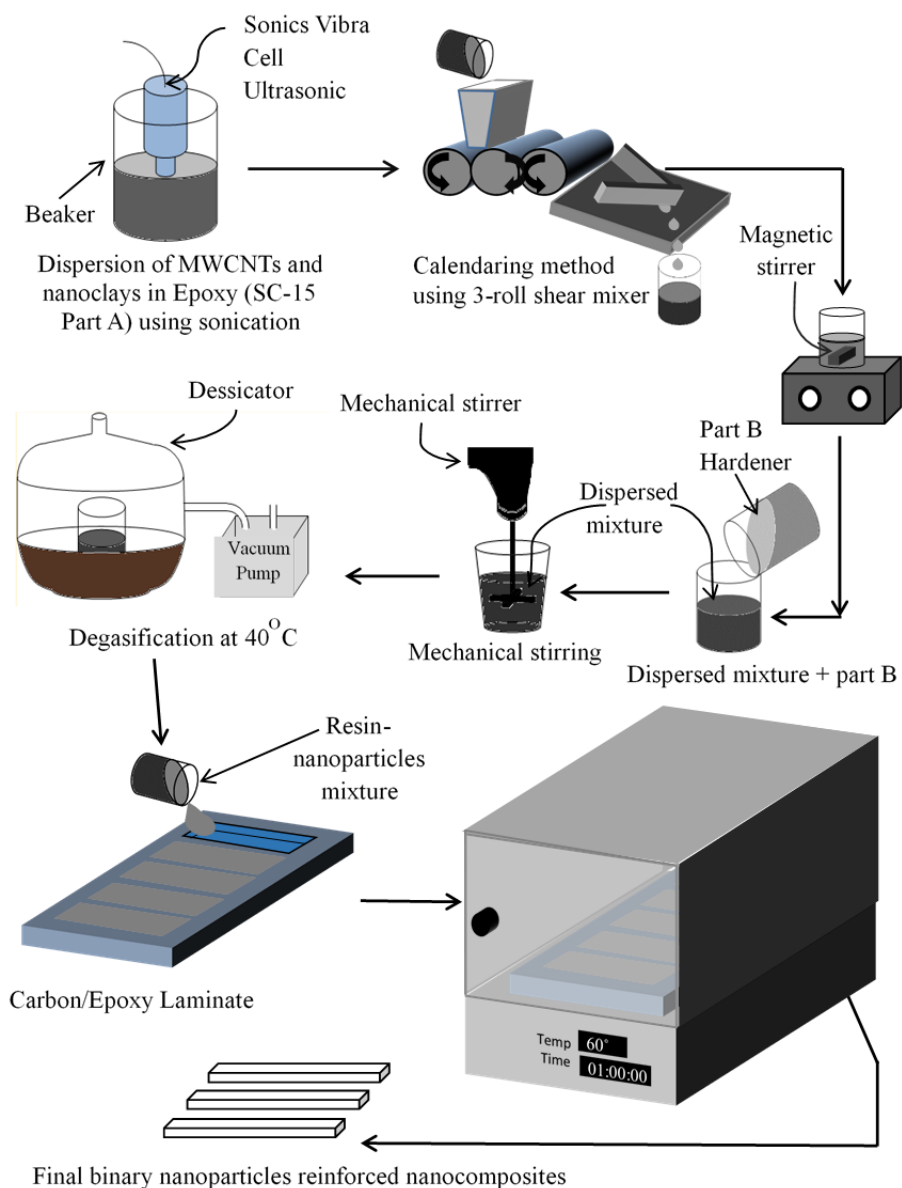
Figure 3.3 fabrication of binary nanoparticles reinforced nanocomposites

3.3.5   Laminate fabrication

After dispersion, part A of SC-15 epoxy containing nanoparticles was mixed with part B at a ratio 10:3. High speed mechanical mixing was done for 10 minutes to obtain a stoichiometric mixture, which was then utilized as matrix for laminates. For control samples, only Part A and part B of SC-15 resin were mixed at a stoichiometric ratio and used as matrix. The resin mixture was degasified at 60°C by placing it in vacuum oven for about half an hour to remove the bubbles formed in the resin due to the mechanical mixing in both cases. Carbon fiber-epoxy nanocomposites were fabricated by a combination of hand lay-up process and compression molding technique. A total of eight layers of woven carbon fabrics was manually impregnated individually with a brush and a roller and then stacked together ensuring proper alignment of fiber tows. The stack was then wrapped with a bleeder cloth and a non-porous Teflon cloth and placed on the platen of a hot press where pressure and temperature were controlled precisely to ascertain maximum wetting of fibers with matrix and compaction of the layup as well as curing. Temperature was kept at 60 °C for 1 hour to attain enough flow of resin at lower viscosity as compared to room temperature and at the same time not to let it flow out of the layup. Temperature was then increased to 120 °C and maintained for 4 hours to obtain completely cured carbon-epoxy composites. Thickness of laminates obtained was about 2.42 mm. Figure 3.4 depicts the fabrication procedure. Coupons of various size according to ASTM standards are cut from the laminated composites to conduct tests.

Sonics Vibra Cell Ultrasonic

Beaker

Dispersion of MWCNTs and nanoclays in Epoxy (SC-15 Part A) using sonication

Calendaring method using 3-roll shear mixer

Magnetic stirrer

Dessicator

Mechanical stirrer

Dispersed mixture

Part B Hardener

Vacuum Pump

Degasification at 40 ºC

Mechanical stirring

Dispersed mixture + part B

Mixture

Carbon fabric

Roller pin

Pressure = 13 tons
Temperature = 120 ºC

Carbon/Epoxy Laminate

254 mm

254

Hot press process for 4 hours.

Final binary nanoparticles reinforced carbon fiber/epoxy samples

Figure 3.4 Fabrication process of binary nanoparticles reinforced carbon fiber/epoxy composites

3.4 Testing procedure

Nanoparticles reinforced nanocomposites and fiber reinforced composites are subjected to various tests to obtain the mechanical, thermal and viscoelastic properties. Properties obtained from composites are compared with the properties obtained from control ones. Moreover microscopic and morphological analysis were performed on fracture surface of the samples.

3.4.1   Fiber Volume Fraction

Fiber volume fraction was computed for fiber reinforced polymer composite (FRPC) samples. Volume fraction of fiber, matrix and void was determined according to ASTM D3171-11. Samples of size 10 mm×10 mm×2.4 mm were cut from the panels and weighed precisely. Samples were then submerged into 80% concentrated nitric acid solution for about 5 hours at a temperature of 75°C to dissolve the matrix. When the matrix was completely dissolved, fibers were washed repeatedly first with acetone and then with water. Fibers were then dried in an oven maintained at 100°C for 1 hours. Weight of dry fibers was measured and volume fraction of fiber, matrix and void was computed.

Fiber volume fraction, $V_f = \frac{W/F}{w/c} \times 100$…………………………………….................(3.1)

Matrix volume fraction, $V_m = \frac{(w-W)/M}{V} \times 100$ …………...…………………........... (3.2)

Void volume fraction, $V_v = 100 - (V_m + V_f)$ ……………………………………..(3.3)

Where,

W= weight of fiber in the composite,

w=weight of the initial composite specimen,

F=density,

M=matrix density,

V=volume of the composite and

C=composite density.

3.4.2 Flexure test

In our research, flexure test was conducted according to ASTM D790-02. The test was conducted in three-point bending configuration using Zwick-Reoll Z 2.5 machine. The test was performed at a rate 1.2mm/minute under displacement control mode. The sample size was maintained according to the ASTM, where span length to thickness ratio is 16:1. Sample size varied for nanocomposites and fiber reinforced composites. For nanocomposites the sample size was 72 mm × 12.5 mm ×4.5 mm whereas for FRPCs the sample size was 40 mm × 12.5 mm × 2.5 mm. At least 5 samples of each type were tested at room temperature. Flexure stress versus strain plot was drawn and flexural modulus was computed from the slope of the initial section of the curve. The flexural strength is calculated from the peak load that the sample can take using homogenous beam theory. Following equations were used to obtain flexural stress, strain and modulus.

$$Flexural\ Strength = \frac{3 \times peak\ load \times span\ length}{2 \times width \times (thickness)^2} \quad \ldots\ldots\ldots\ldots\ldots\ldots\ldots\ldots\ldots\ldots\ldots\ldots\ldots\ldots\ldots\ (3.4)$$

$$Flexural\ strain = \frac{6 \times maximum\ deflection\ at\ center \times thickness}{span\ length^2} \quad \ldots\ldots\ldots\ldots\ldots\ldots\ldots\ldots\ldots\ldots(3.5)$$

$$Flexural\ Modulus = \frac{Slope\ of\ tangent \times (span\ length)^2}{4 \times width \times (thickness)^2} \quad \ldots\ldots\ldots\ldots\ldots\ldots\ldots\ldots\ldots\ldots\ldots.....(3.6)$$

3.4.3 Tensile test

Tensile test was conducted on fiber reinforced polymer composites according to ASTM standard D3039. Rectangular samples were cut from the composite panels at 200 mm × 20 mm × 2.5 mm size. The tests were conducted in MTS 809 Axial/Torsional Test System machine equipped with 100N load cell. The tests were performed in displacement control mode at a rate 2 mm/minute. The tensile fatigue test was also performed in this research. 1 wt. % and 2 wt. % nanoclay reinforced as well as control carbon fiber/epoxy composites are subjected to fatigue tensile testing. The fatigue tensile test were performed in force control mode at loads equivalent to 90%, 80% and 70% stress of ultimate strength. The minimum to maximum stress ratio, R was 0.1.

Fatigue life is assumed to be normally distributed and variance of log of life cycle over the entire range was constant. It is assumed that the fatigue life is normally distributed. Log normally distributed S-N curves can be expressed as,

$$Y = A + BX \ldots\ldots\ldots\ldots\ldots\ldots..\ldots\ldots\ldots\ldots\ldots\ldots\ldots\ldots\ldots\ldots\ldots\ldots\ldots\ldots\ldots\ldots\ldots.(3.7)$$

Where,   Y=log (N); N= Number of cycles the sample run.

        X is the maximum cyclic stress

and   A and B are constants for each sample estimated by equation (2).

$$\hat{A} = \bar{Y} - \hat{B}\bar{X} \ldots\ldots\ldots\ldots\ldots\ldots\ldots\ldots.\ldots\ldots\ldots\ldots\ldots\ldots\ldots\ldots\ldots\ldots\ldots\ldots\ldots\ldots\ldots\ldots...\ldots.(3.8)$$

and

$$\hat{B} = \frac{\sum_{i=1}^{k}(X_i - \bar{X})(Y_i - \bar{Y})}{\sum_{i=1}^{k}(X_i - \bar{X})^2} \dots\dots\dots\dots\dots\dots\dots\dots\dots\dots\dots\dots\dots\dots(3.9)$$

Here, (^) denotes estimators and (‾) denotes average values. K is the number of samples involved in each test program. The variance in data is estimated by, σ^2 which can be calculated by,

$$\sigma^2 = \frac{\sum_{i=1}^{k}(Y_i - \hat{Y})^2}{k-2} \dots\dots\dots\dots\dots\dots\dots\dots\dots\dots\dots\dots\dots\dots(3.10)$$

Where, Y the estimated fatigue life from the median S–N curve.

3.4.4 Dynamic Mechanical Analysis

Viscoelastic properties of both nanocomposites and fiber reinforced composites are obtained from dynamic mechanical analysis. DMA tests were conducted according to ASTM D4065 using TA instrument DMA Q 800. The tests were performed in three point bending mode at a frequency 1 Hz and amplitude 15 μm. The temperature ramp was 10°C/minute within the range 30°C and 180°C. The sample size was 60mm×13mm×3mm for the test. Storage modulus, loss modulus and tan-delta as a function of temperature are obtained from dynamic mechanical analysis. Glass transition temperature is considered as the temperature corresponding to the tan-delta curve peak. Crosslink density can be computed from the result obtained.

$$\lambda = G/RT \quad \dots\dots\dots\dots\dots\dots\dots\dots\dots\dots\dots\dots\dots\dots\dots(3.11)$$

Where,

λ = Crosslink density,

G= Storage modulus in rubbery plateau region,

R= Universal gas constant,

T= absolute temperature in Kelvin.

3.4.5 Thermo-mechanical Analysis

Thermo-mechanical analysis was conducted to obtain the coefficient of thermal expansion from samples. Both nanocomposites and fiber reinforced composites are subjected to thermo-mechanical analysis. The test was done according to ASTM D696. Nanocomposites are isotropic materials, test conducted in any direction resulted in same result. For fiber reinforced composites, the test was conducted along the axis and through thickness direction. TA instrument Q 400 was used to conduct the test in expansion mode. The temperature ramp was 10 °C/minute within the range 30 °C and 180 °C. The system is purged by liquid nitrogen gas at a flow rate of 50 ml/minute. Sample size varied for nanocomposites and FRPCs. Dimension change versus temperature curve was obtained from the test. Glass transition temperature can be obtained from the plot. From the slope of the curve and initial length of the specimen, coefficient of thermal expansion before and after glass transition temperature is computed.

$$Coefficient\ of\ thermal\ expansion, \propto = \frac{1}{L} \times \frac{dL}{dt}$$ …………………………………..(3.12)

Where,

L=initial length of sample.

dL/dt = slope of dimension change versus temperature plot.

3.4.6 Morphological Study

Scanning electron microscopic analyses were performed to analyze the fracture mode at higher magnification. Analysis of fracture surfaces was carried out using a JEOL JSM-6400 scanning electron microscope (SEM) at 15 kV accelerating voltage. Specimen surfaces were coated with a thin gold film for SEM observation. One sample from each set impacted at 30 J was observed under scanning electron microscopy to understand failure behavior at various magnifications.

3.4.7 Optical Microscopy

To obtain qualitative information about the damage of the specimens tested, specimens were observed through optical microscope model Unitron ZST (Zoom Stereo Trinocular) from Excel Technologies INC. From three samples of each type tested at varied energy level one sample was cut into two halves to observe the cross-section.

3.5 Summery

In this research, epoxy SC-15 and carbon fiber/ epoxy composites were modified with binary nanoparticles. Nanocomposites and fiber reinforced composites with and without nanoparticles were subjected to mechanical test, dynamic mechanical analysis, thermomechanical analysis and morphological analysis. Transisnt data from these tests were accumulated to calculate mechanical, thermal and viscoelastic properties.

4. CHAPTER IV NANOCOMPOSITES CHARACTERIZATION

4.1 Introduction

Nanocomposites reinforced with MWCNTs, nanoclays and binary nanoparticles were subjected to flexure, dynamic mechanical analysis and thermomechanical analysis to obtain mechanical, viscoelastic and thermal properties. Transient results from these tests were accumulated. Mechanical properties such as flexural and tensile strength, modulus and strain were computed from the obtained data. Viscoelastic properties such as storage modulus, loss modulus and tan-delta were plotted as a function of temperature. Thermal properties like glass transition temperature, coefficient of thermal expansion were also calculated. Mechanical, thermomechanical and viscoelastic properties for nanoparticles reinforced composites were compared with the properties obtained from control ones. Fracture surfaces of all types of samples were analyzed under optical microscope and scanning electron microscope.

4.2 FTIR analysis

FTIR analysis was performed to observe the effect of various nanoparticles on the epoxy SC-15 resin and to understand the chemical reactions, taken place in time of curing. Chemical structure of byproducts from the reaction of part A and part B while curing was depicted in spectrum for control epoxy resin. Likewise, if new byproducts were produced at the time of curing while nanoparticles had been added, their characteristic peaks would be present in the spectrum. Characteristic bands for epoxy SC-15 resin were exhibited at different wavelength in the spectra depicted in Figure 4.1. The presence and intensity of peaks varied with the

addition of nanoparticles. Due to the C-O stretching of saturated aliphatic primary alcohols peaks at wavenumbers 1032 cm^{-1} and 1095 cm^{-1} are exhibited (Tcherbi-Narteh et al., 2013). Intensity of these peaks decreases with the addition of nanoparticles. The characteristic peaks at wavenumbers 1454 cm^{-1} and 1508 cm^{-1} represent aromatic ring stretching of carbon-carbon double bonds. The peak at 1508 cm^{-1} at wavenumber can be attributed to NH$_2$ group present in cycloaliphatic amine curing agent. Peaks for nanocomposite samples exhibited restrictive stretching compared to the peaks of control samples. The peaks at wavenumber 1236 cm^{-1} and 932 cm^{-1} represent stretching of epoxide bond and peak at 823 cm^{-1} represents stretching of C-O-C present in epoxy SC-15 (Alamri & Low, 2013). Peaks were observed at wavelength 2860 cm^{-1} and 2902 cm^{-1} due to C-H stretching of epoxy SC-15 resin, but the intensity of peaks decreases with the addition of nanoparticles. A broad peak was observed in the range 3100-3600 cm^{-1} for neat epoxy resin due tothehydroxyl group in cured epoxy and N-H stretching of amine hardener. Due to the addition of nanoparticles, some unreacted primary amine group from hardener may be present in nanocomposites, which is depicted by doublet in 3600 cm^{-1} region. Specially, in case of nanoclays reinforced nanocomposites unreacted primary amine group is present, which is harmonious with the reaction mechanism in the next section. Moreover, carboxyl functionalized MWCNTs might have reacted with part B of epoxy SC-15 and formed amide group resulting in a peak at wavelength 1680 cm^{-1} for both MWCNTs and binary nanoparticles reinforced nanocomposites.
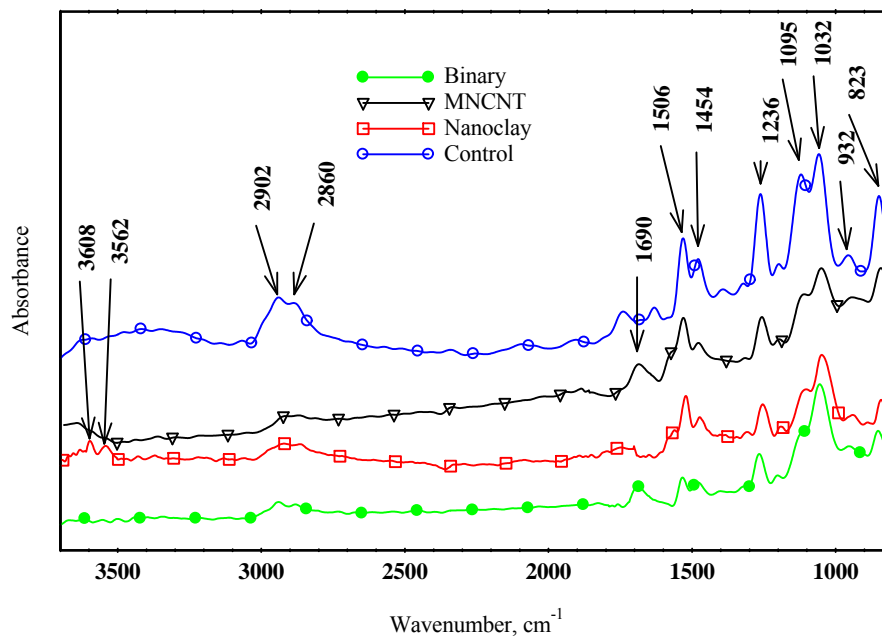
Figure 4.1 FTIR spectrum of nanoparticles reinforced and control nanocomposites

4.2.1   Reaction Mechanism

Epoxy SC-15 is a two part thermoset polymer. Part A contains Diglycidyl ether of bisphenol A and part B contains hardener that is cycloaliphatic amine. The chemical structure of Epoxy part A and part B is depicted in figure 3.1. Epoxy SC-15 part A contains epoxide ring that reacts with amine group present in the part B. The reaction mechanism is portrayed in figure 4.2. Every epoxy molecule is connected with other epoxy molecules forming a huge epoxy network. It is called the cross-linking of epoxy resin. When part A is mixed with part B in

stoichiometric ratio 10:3, there is exact amount of amine group in part B to take part in ring

opening reaction with epoxide group present in part A of the resin.
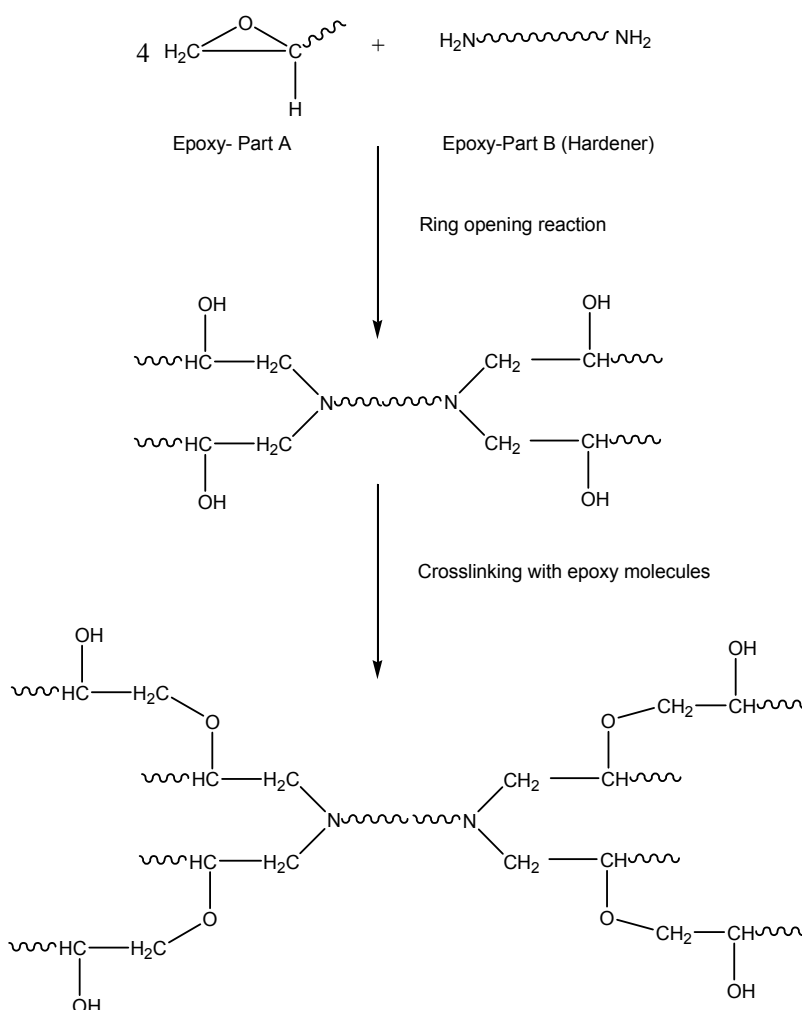
Figure 4.2 Epoxy SC-15 part A and part B hardener reaction mechanism

In this research, nanoparticles were added with epoxy resin as reinforcement. MWCNTs

were COOH group functionalized whereas, nanoclays were modified with octadecylamine.

Thus when these nanoparticles were added to epoxy they were supposed to react with the

resin. From FTIR analysis, we can also observe the difference in spectra of nanocomposites

compared to control resin. The probable reactions are shown in figure 4.3 and 4.4. When

nanoclays were infused in resin, the I-30E nanoparticles supplied amine functional group in addition to the amine groups present in part B of epoxy resin. The amine functional group present in nanoclays might have reacted with part A of epoxy system and ring opening reactions might take place as shown in figure 4.3. As a result, the nanoclays might have chemically interact with the epoxy resin. The epoxide group on the other end of the epoxy chain reacted with amine group of part B. Opposite end of part B reacted with another epoxy molecule and formed resin-nanoclays network instead of only resin network obtained for control epoxy resin. Thus, functionalized nanoclays took part in the formation of matrix network through cross-linking. The abundant amine functional groups disrupted the stoichiometric ratio for reaction. Therefore, unreacted part B might be present in the system. Observation from FTIR spectrum of nanoclays reinforced nanocomposites supports this phenomenon where, abundant amine functional groups are observed (figure 4.1). On the contrary, MWCNT used in this research is carboxyl functionalized. Epoxy ring–opening reaction requires strong nucleophile. Carboxyl groups are not nucleophile. Thus, they do not react with part A of SC-15 epoxy resin. Yet, part B of Epoxy SC-15 resin is a di-amine product. Therefore, carboxylic groups of MWCNTs might have reacted with amine groups present in epoxy SC-15 part B as shown in figure 4.4. The amine group present in the opposite end of di-amine hardener worked as a nucleophile and took part in epoxide ring opening. Thus, MWCNTs might have reacted with the epoxy system and took part in the cross-linking. Thus, there might be a shortage of amine group to take part in reaction with part A. Both the above mentioned reaction mechanism is applicable for binary nanoparticles reinforced composites. The octadecylamine surface modified nanoclays reacted with part A

of epoxy and carboxyl functionalized MWCNTs reacted with part B of epoxy followed by the epoxy molecules connecting through ring opening reaction. A MWCNTs-nanoclays-resin network might have formed due to binary nanoparticles reinforcement. Carboxyl functionalized MWCNT reacting with part B may facilitates to balance the abundant amine functional group resulted from interaction between octadecylamine modified nanoclays and epoxy part A. This phenomenon explains the absence of peaks for primary amine group in FTIR spectrum of binary nanoparticles reinforced nanocomposites.
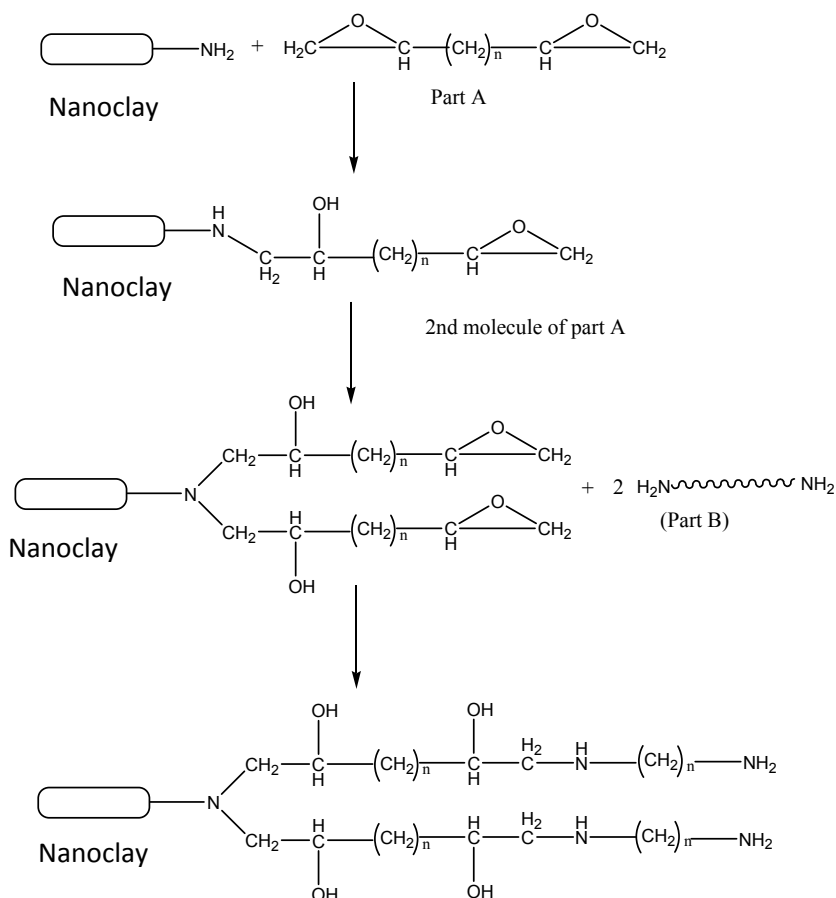
Figure 4.3 Probable chemical reaction between epoxy SC-15 and octadecylamine surface modified I-30E nanoclay
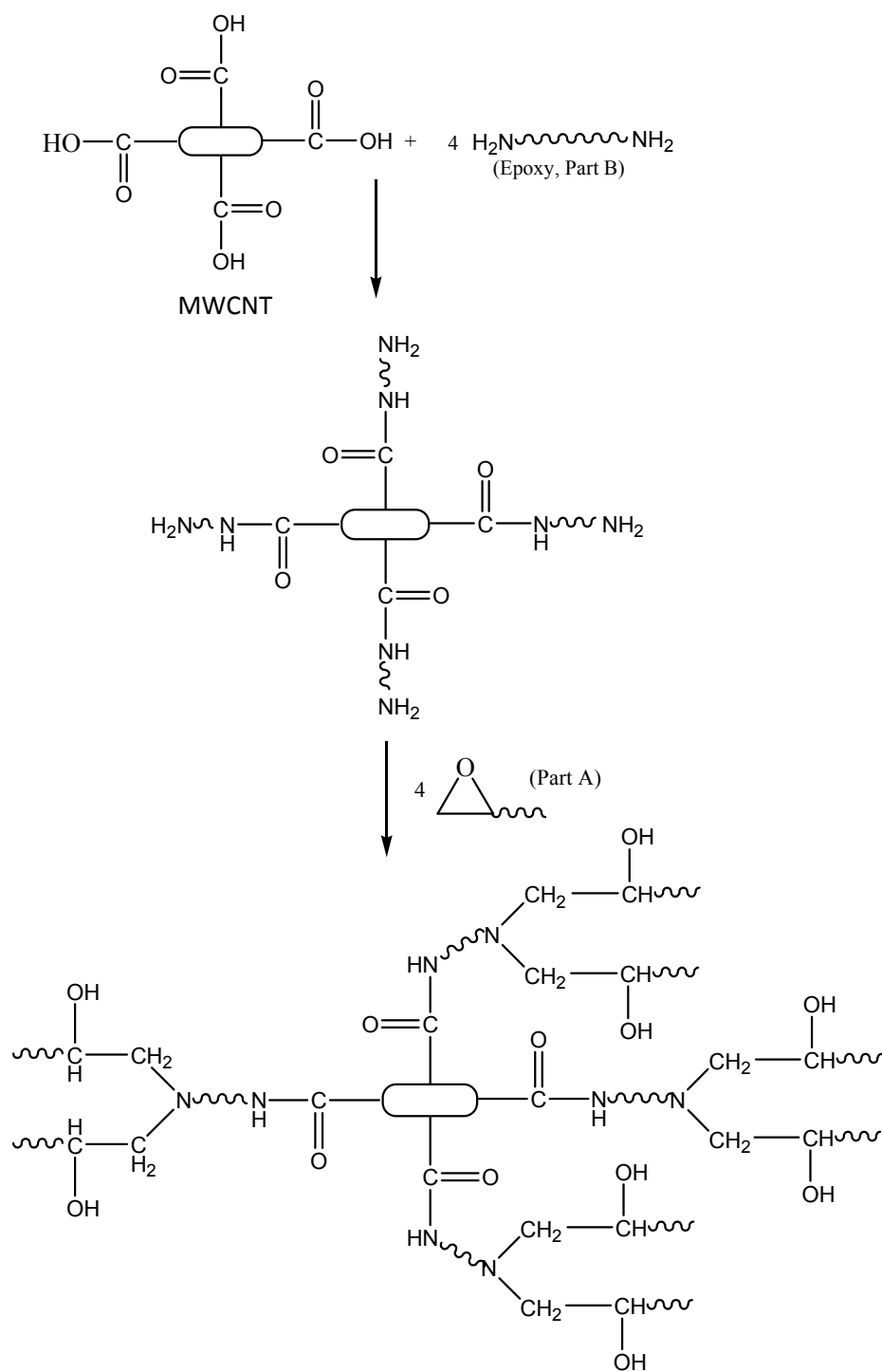
Figure 4.4 Probable chemical reaction between epoxy SC-15 and carboxyl functionalized

MWCNTs

4.3 Flexural Properties of Nanocomposites

Characterization of flexural properties of nanocomposites is conducted by subjecting MWCNTs, nanoclays and binary nanoparticles reinforced samples as well as control SC-15 epoxy resin samples under three point bending load. Nanocomposites were fabricated according to the size indicated in ASTM standards. The samples were subjected to three point bending load and transient data were accumulated. Flexure stress, strain and modulus were computed according to the equations illustrated in Chapter 3. Comparison of flexural test results from various samples is presented in figures 4.5-4.6 and table 4.1.
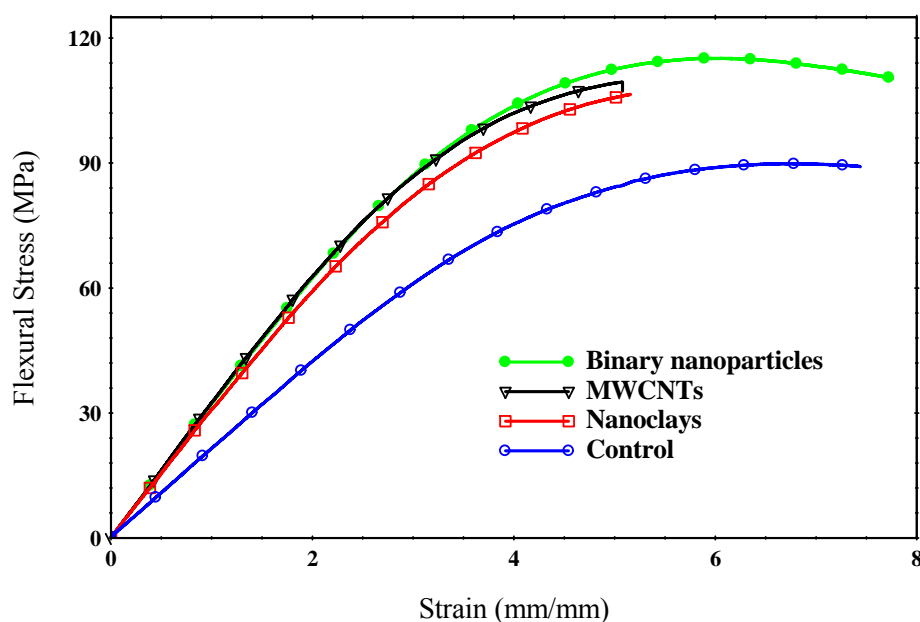
Figure 4.5 Flexural Stress versus strain response of control and nanoparticles reinfroced nanocomposite samples

Table 4.1 Flexure test results of control and nanocomposites

Sample type	Flexural Strength (MPa)	% Improved	Flexural Modulus (GPa)	% Improved	Strain at maximum load (mm/mm)	% Improved
Control	89.56±2.39	-	2.21±0.14	-	5.81±.82	-
Nanoclay Reinforced	106.58±0.94	19	2.98±0.12	35	5.53±0.66	-4
MWCNT reinforced	109.85±1.03	23	3.14±0.17	42	5.58±0.57	-4
Binary nanoparticles reinforced	**115.62±0.99**	**29**	**3.18±0.08**	**44**	**5.86±0.42**	**1**

The effect of the nanoparticles infusion is evident from figure 4.5 and table 1. All nanoparticles incorporated samples exhibited significant improvement of flexural strength and modulus. Nanoclays and MWCNTs reinforcement yielded an increase of 19% and 23% in flexural strength and 35% and 42% in flexural modulus respectively. A maximum increase of 29% and 44% in flexural strength and flexural modulus for binary nanoparticles reinforced samples was observed compared to control samples. Figure 4.6 exhibits the comparison of flexural strength and modulus among different samples. In case of strain at maximum load, no significant difference was observed among the samples. Increase in flexural strength and modulus can be attributed to nanoparticles infusion in epoxy SC-15 resin. Previous researches revealed the influence of nanoparticles on epoxy SC-15 resin (M. M. Rahman et al., 2012; Salam et al., 2013).
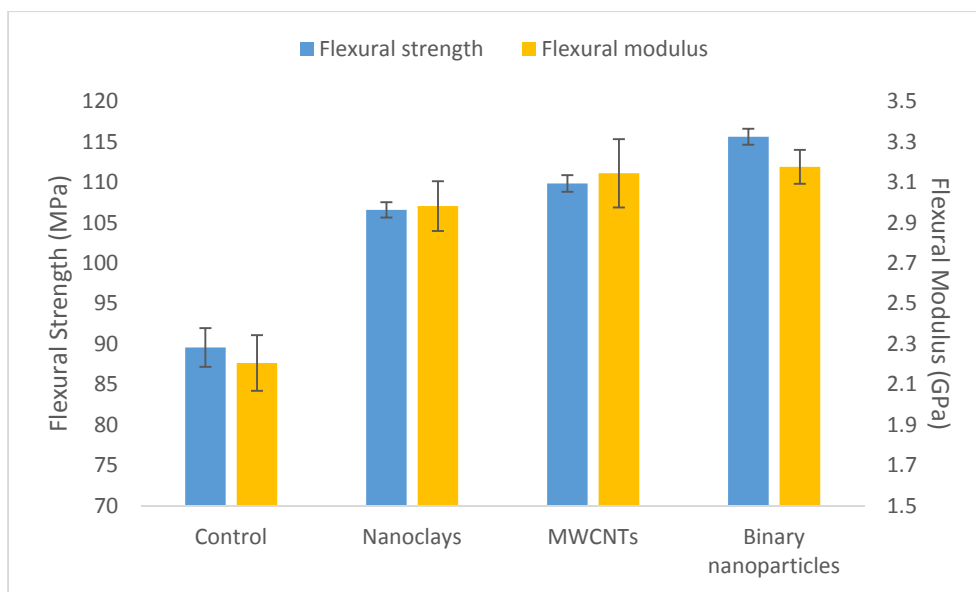
Figure 4.6 Comparison of flexural strength and modulus exhibited by nanoparticles

reinforced and control nanocomposites samples

Uniform dispersion of nanoparticles ensures more viable sites for polymer and nanoparticles interaction. Amino functional groups are present in the surface of I.30E montmorillonite nanoclays modified with 25-30% Octadecylamine. Amino functional groups are strong nucleophile. Therefore, these amino functional groups of nanoclays and epoxide group of epoxy SC-15 reacts and form strong covalent bond. When nanoclays are dispersed in part A of epoxy SC-15, ring opening reactions take place followed by higher cross-linking between epoxy molecules depicted in figure 4.3. Higher cross-link reaction results in interlocking resin-nanoparticles structure in matrix, which reduces the mobility of epoxy polymer chains. On the contrary, MWCNT used in this research is carboxyl functionalized. The proposed reaction mechanism of carboxyl functionalized MWCNT and part B of Epoxy SC-15 resin is depicted in figure 4.4. MWCNTs react with amine functional group of part B of epoxy SC-15

thereby, taking place in the epoxy resin-nanoparticles matrix structure when cured. In case of binary nanoparticles both mechanism play role in forming the resin-nanoparticles matrix structure. Chemically interlocked resin and nanoparticles structure may facilitate stress transfer when loaded.

Uniform dispersion of nanoparticles in resin is very important to enhance the properties of nanocomposites. Uniform dispersion ensures more surface area of nanoparticles open to resin. This facilitates the functional groups on the surface of nanoparticles to be exposed to epoxy molecules resulting in crosslinking between nanoparticles and resin. Crosslinking between resin and nanoparticles may facilitate the stress transfer from resin to nanoparticles. High strength and stiffness as well as high aspect ratio of MWCNTs made them very useful to carry high loads while reinforced to resin.

Nanoclays are layered structures. Proper dispersion of nanoclays can be achieved by exfoliation of nanoparticles. Exfoliation is the infusion of resin between two layers of nanoclays structure, so that they transform into flexible single layered structure. Sometimes the nanoparticles are intercalated between the layers of nanoclay structure. More exfoliated structure is desired for enhancement of properties as more resin between two layers ensure more reaction sites for cross-linking. Moreover, the layers of nanoclay structures act as reinforcing plates to resin structure. In case of binary nanoparticles, both nanoparticles come into play. Physically the nanoparticles stay side by side to reinforce the resin system. Epoxy resin, nanoclays and MWCNT forms a network which is bonded by strong covalent bonds together. When the nanocomposites are subjected to loading, these strong covalent bonds must be severed before the sample fails. Higher cross-linking ensures higher amount of

covalent bonds to severe when subjected under load. Thus, flexure strength and modulus of nanoparticles reinforced composites may have increased.

Flexural strain of nanocomposites remained almost same with the addition of nanoparticles, with maximum increase of 1% for binary nanoparticles reinforced composites shown in figure 4.5. Fracture energy of nanocomposites can be enhanced by reinforcing it with nanoparticles. After initiation of crack due to loading, the propagation of crack can be arrested by the presence of nanoparticles. As the crack faces nanoparticles in the propagating direction, it has to change the direction. Thus, presence of nanoparticles ensures the change in the direction of crack propagation. The morphological study on the fracture surface of control and nanocomposites samples are presented in figure 4.28. It is evident from the images that, the fracture surface of nanocomposites are rougher than the control samples. Among the nanocomposites, binary nanoparticles reinforced ones exhibit most rough fracture surface. This direction change requires more energy, which enables the nanocomposite samples to carry higher load. Likewise, strain to failure also increase with addition of nanoparticles. Binary nanoparticles reinforced nanocomposites have more nanoparticles that faces the crack fronts compared to single nanoparticles reinforced nanocomposites making them more effective in arresting crack propagation.

4.4 DMA of Nanocomposites

Dynamic mechanical analysis provides the viscoelastic properties of composite samples as a function of temperature. Unmodified epoxy resin as well as MWCNTs, nanoclays and binary nanoparticles modified nanocomposites were subjected to dynamic mechanical analysis to

observe the effect of nanoparticles on stiffness of composites. Figure 4.7-4.9 depict the variation of dynamic mechanical parameters such as storage modulus, loss modulus and tan-delta as a function of temperature. All data accumulated are presented in table 2. Figure 4.7 depicts variation of storage modulus with incorporation of nanoparticles. Likewise, figure 4.8 and figure 4.9 show the variation of loss modulus and tan-delta with incorporation of nanoparticles. Binary nanoparticles contains 2 wt. % of nanoclays and 0.1 wt. % of MWCNTs, whereas MWCNTs reinforced nanocomposites contain 0.3 wt. % of MWCNTs and nanoclays reinforced nanocomposites contain 2 wt. % nanoclays.
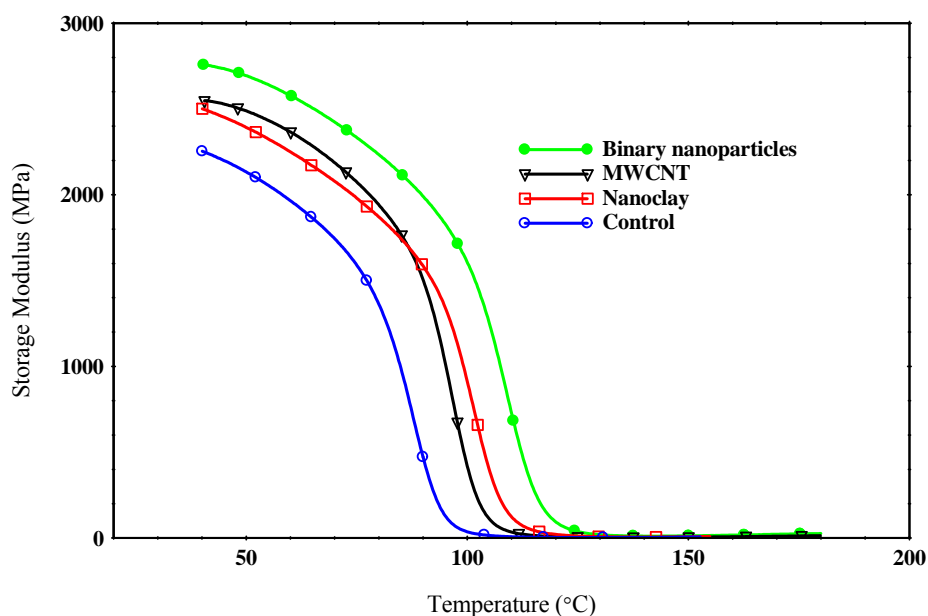
Figure 4.7 Storage modulus of nanoparticles reinforced and control epoxy composites from dynamic mechanical analysis
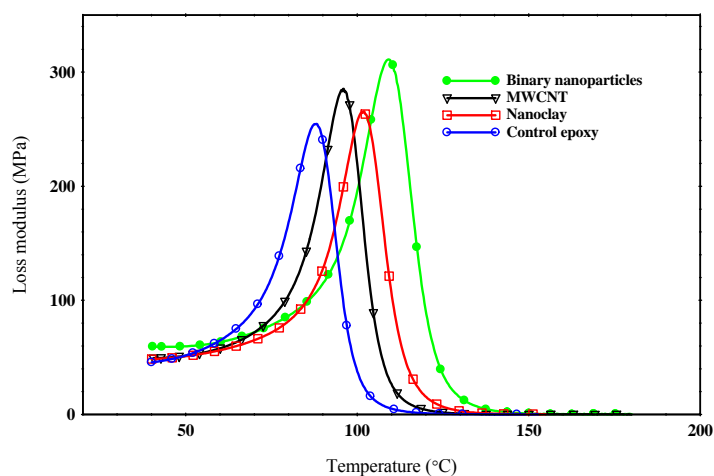
Figure 4.8 Loss modulus of nanoparticles reinforced and control epoxy composites from

dynamic mechanical analysis

Figure 4.9 Tan-delta of nanoparticles reinforced and control epoxy composites from dynamic

mechanical analysis
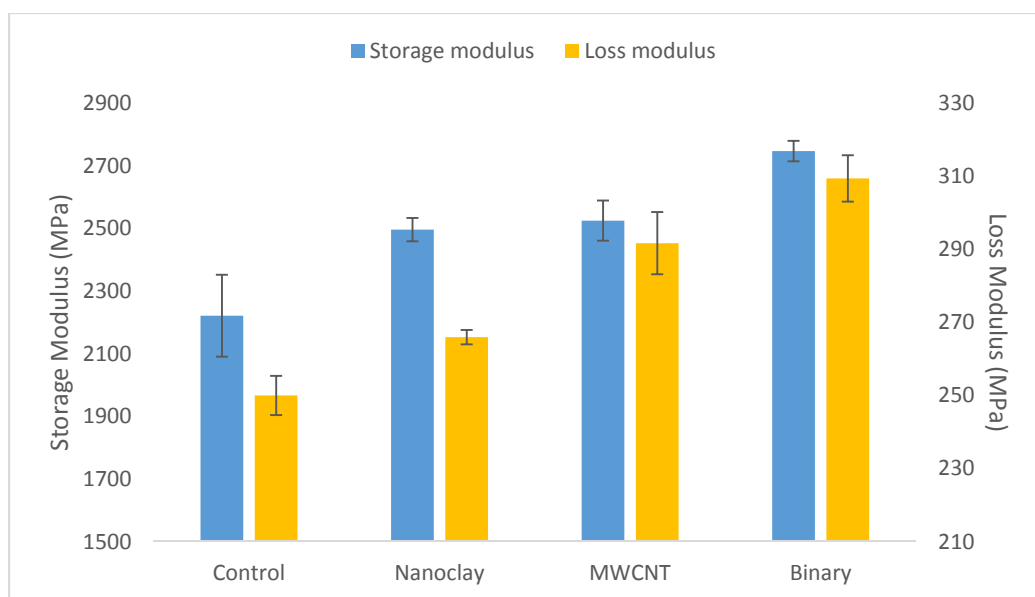
Figure 4.10 Comparison of storage and loss modulus for nanoparticles reinforced epoxy

nanocomposite with epoxy resin

Table 4.2 DMA results of control and nanocomposites

Sample Type	Storage modulus (MPa)	% Change	Loss modulus (MPa)	% Change	Glass Transition Temperature	% Change	Crosslink density ($\times 10^{-3}$ mol.cm^{-3})
Control epoxy resin	2221.67 ± 130.85	-	250 ± 35.38	-	99.08 ± 0.75	-	1.03
Nanoclays reinforced nanocomposites	2496.33 ± 37.22	12	265.97 ± 1.97	6	113.62 ± 1.55	14	1.59
MWCNTs reinforced nanocomposites	2525.33 ± 64.08	14	291.7 ± 8.53	16	106.94 ± 1.17	7	1.19
Binary nanoparticles reinforced nanocomposites	2747.33 ± 32.59	24	309.42 ± 6.35	24	122.82 ± 1.77	23	3.23

4.4.1 Storage modulus

Storage modulus represents the energy stored in the composites after deformation under load. In dynamic mechanical analysis storage modulus of composites is recorded while the specimen is subjected under cyclic loading at varying temperature. Figure 4.7 depicts storage modulus of all types of composite samples as a function of temperature and figure 4.10 exhibits the comparison of storage modulus for all samples.

It is evident from figure 4.10 that, storage modulus has increased due to the addition of nanoparticles in almost all temperature regions. In the glassy region that is before the glass transition temperature, significant increase in storage modulus was observed, whereas after glass transition temperature at rubbery region storage modulus increased slightly. From flexure and tensile test results, it is evident that binary nanoparticles reinforcement enhances modulus of composites significantly. Thus at room temperature, the storage modulus exhibited by MWCNTs, nanoclays and binary nanoparticles reinforced nanocomposites are 13%, 14% and 27% higher than the storage modulus exhibited by control ones. As the temperature increases, the epoxy polymer chain starts to move. At first the side chains start to move followed by large chains. Due to polymer chain movement, the composite loses stiffness. In case of nanocomposites, the resin network is replaced with resin-nanoparticles network. A well dispersed nanoparticles in resin network might have restricted the movement of polymer chain around the nanoparticles below glass transition temperature. Also exfoliation of layered structure nanoclays strengthen resin as matrix material. Thus, the enhancement of storage modulus can be attributed to uniform dispersion of nanoparticles in

the nanocomposites. Above glass transition temperature in rubbery region slight increase in storage modulus was exhibited by nanoparticles reinforced composites. In rubbery region, molecular motion increases along with higher amplitude for which less or no contact between macromolecule and nanoparticles results in lack of shear force between macromolecules (Montazeri & Chitsazzadeh, 2014). Generally, the operating temperature of composite structures are under glass transition temperature. Thus, nanoparticles are highly effective to increase the storage modulus of composites.

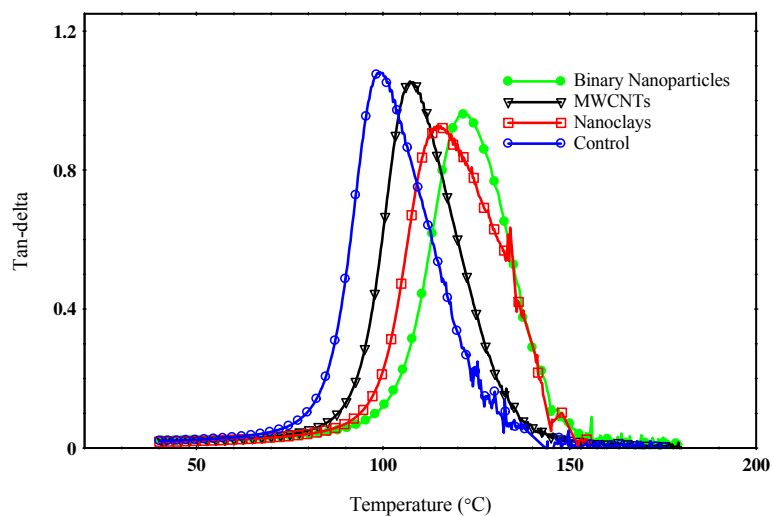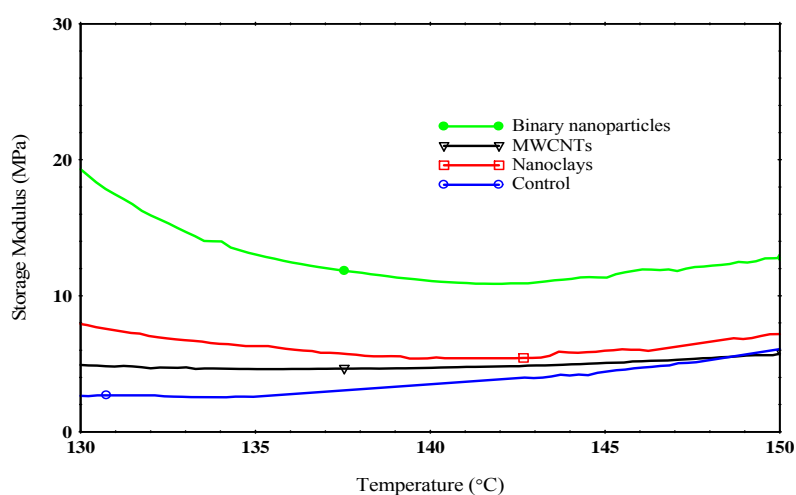Figure 4.11 Storage modulus of rubbery plateau region of nanoparticles reinforced and control epoxy composites from dynamic mechanical analysis

Figure 4.11 depicts storage modulus of rubbery plateau region of nanocomposites and control epoxy. Nanoparticles can influence the storage modulus in rubbery region. Binary nanoparticles reinforced nanocomposites exhibit highest storage modulus. The value of storage modulus from rubbery plateau region was used to compute cross-link density of

nanocomposites with the equation 3.4. Cross-link density values are accumulated in table 2. From table 2, it is evident that cross-link density in binary nanoparticles reinforced nanocomposites are three times higher than the cross-link density of control epoxy. Higher cross-link density ensures higher stiffness due to more rigid structure. Moreover, it ensures more interaction between nanoparticles and resin as stated in section 4.2.

4.4.2   Loss modulus

Loss modulus represents the energy dissipated into heat when deformed under load. It indicates the viscous component of a viscoelastic materials. When subjected under cyclic loading, it is the unrecoverable dissipated energy per cycle. Figure 4.10 portrays loss modulus for unmodified and nanoparticles modified composite samples. For all composite samples, loss modulus increases with temperature up to glass transition temperature, then decreases with further increase of temperature. Temperature associated with the peak of loss modulus represents the glass transition temperature indicating change of glassy state to rubbery state. Glass transition temperature obtained form loss modulus curve is said to be much more realistic than those found from damping factor curves. Figure 4.12 contains T_g values obtained from loss modulus and damping factor respectively, where T_g values from loss modulus plots are lower than those from damping factor plots. T_g values are higher for nanoparticles modified composites compared to those of control ones. For binary nanoparticles modified composites loss modulus is highest. Uniform distribution of nanotubes offers high resistance against the movement of surrounding matrix resulting in high dissipation of energy (M. M. Rahman et al., 2013). Moreover, exfoliation and intercalation of nanoclays allows the resin to reside in nanoclay layers, thereby strengthening

the matrix. Thus, to deform the composites more energy dissipation occurs in case of binary nanoparticles reinforced composites compared to the composites modified with only nanoclays or MWCNTs.
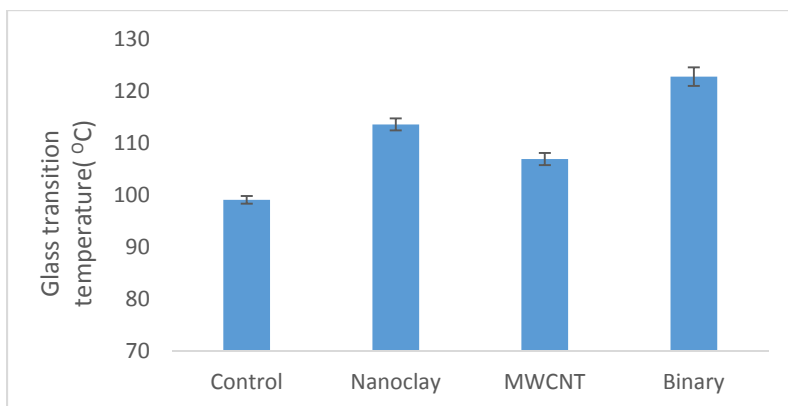
Figure 4.12 Comparison of glass transition temperature for nanoparticles reinforced epoxy nanocomposites with epoxy resin

4.4.3 Damping properties

Tan-delta values can be obtained from the ratio of loss modulus over storage modulus Higher value of tan-delta ensures better damping properties. From figure 4.9, it is evident that, tan-delta values are higher for nanoparticles reinforced composites. Glass transition temperature can be obtained from the peak of tan-delta curve. Glass transition temperature for binary nanoparticles reinforced composites increases 23% compared to control samples. Nanoparticles in nanocomposites restrict the molecular motion of polymer chains when the temperature increases. Thus the polymer chains in resin- nanoparticles network starts to move at a higher temperature than the polymer chains of the control resin samples, resulting in high glass transition temperature.

4.5 Thermo-mechanical analysis of nanocomposites

Figure 4.13 exhibits the dimension change versus temperature plot for nanocomposites. From the slope of the plot and initial length of nanocomposites coefficient of thermal expansion can be obtained. From figure 4.13, it is evident that, the nanocomposites expand with the increase of temperature up to glass transition temperature. When the transition starts, the nanocomposites transforms from glassy state to rubbery state. So, the nanocomposites softens and the probe measuring the dimension drops down. A sharp drop of the plot can be observed at onset of glass transition. So the dimension decreases. The dimension decreases until the transition finishes and the nanocomposite becomes rubbery. Then the probe reaches the lowest point. That's the lowest point on plot. After that, with increase of temperature the dimension increases. From these two parts of the plot, that is before and after glass transition temperature, slope of the plot are recorded and from the slope and initial length of composite coefficient of thermal expansion can be obtained.
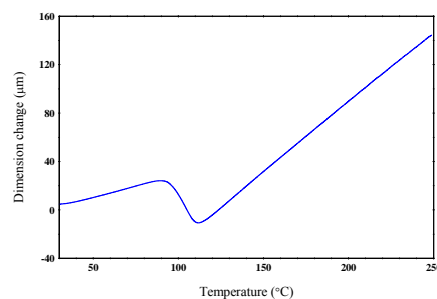
Figure 4.13 Sample dimension change versus tmperature plot for binary nanoparticles reinforced nanocomposites.

Figure 4.14 depicts comparison between CTE values obtained from control and nanocomposite samples before and after glass transition temperature. All nanoparticles reinforced carbon fiber/epoxy samples exhibits lower CTE than control ones before and after glass transition. Nanoparticles form covalent bonds with epoxy resins forming epoxy-nanoparticles network as shown in section 4.1. This network reduces the mobility of epoxy polymers forming resin-nanoparticles network. Moreover, at high temperature lower energy is needed to degrade control epoxy composites. Due to resin-nanoparticles network, higher energy is required to degrade nanocomposites, so degradation starts at later temperature. For binary nanoparticles, more reaction between nanoparticles and resin lead to stronger network of matrix reducing the mobility to higher extant. The CTE of binary nanoparticles reinforced samples are minimum. After glass transition temperature, the samples became rubbery from glassy. Thus, the resistance to deform due to the presence of nanoparticles became less effective. Therefore, CTE values after glass transition temperature is much less influenced by nanoparticles as shown in table 4.3.
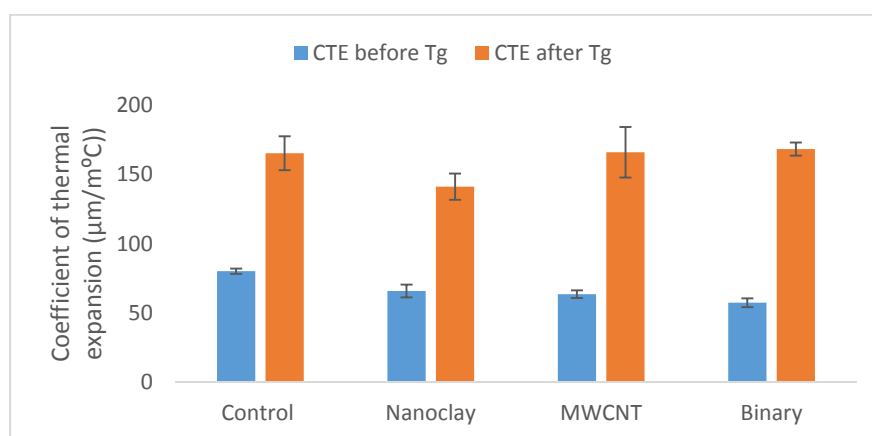
Figure 4.14 Coefficients of thermal expansion before and after glass transition temperature for nanocomposites

Glass transition temperature of samples obtained from thermomechanical analysis were compared in figure 4.15. Glass transition temperature for binary nanoparticles reinforced nanocomposites increased about 24% compared to control epoxy resin, which is analogous to glass transition temperature results obtained from dynamic mechanical analysis.
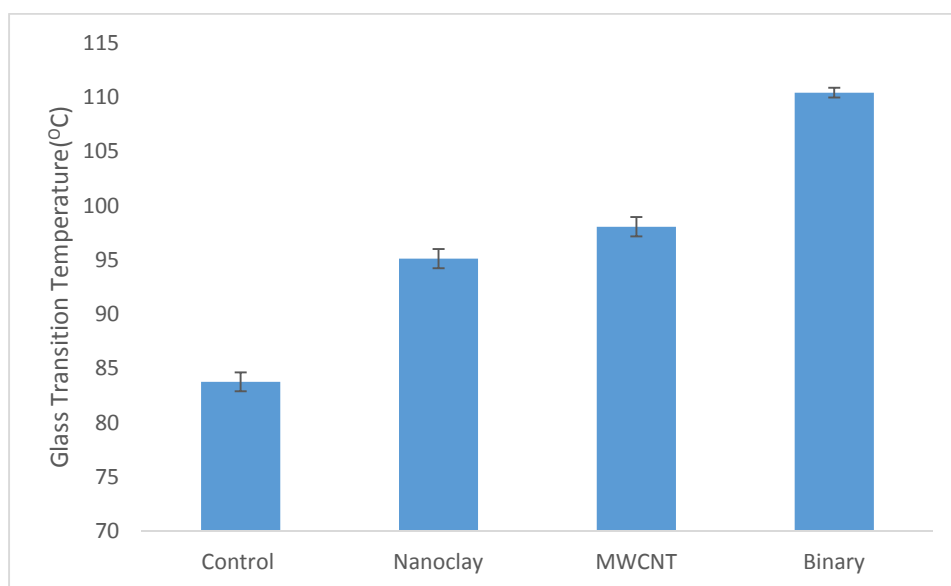
Figure 4.15 Glass transition temperature of nanocomposites from TMA

Table 4.3 TMA results for nanocomposites

Sample Type	CTE before T_g	% Improvement	CTE after T_g	% Improvement	T_g	% Improvement
Control	80.08±1.9	-	165.24±12.23	-	83.77±0.87	-
Nanoclay reinforced	65.78±4.67	20	141.07±9.49	15	95.13±0.88	7
MWCNT reinforced	63.49±2.81	21	165.902±18.25	1	98.07±0.89	13
Binary nanoparticle	57.3±3.18	30	168.2±4.71	1	110.42±0.45	24

4.6 Microscopic analysis of nanocomposites

Flexure test of nanocomposites resulted in failure of nanocomposites. All the samples were fractured due the three-point bending load. The fractured surfaces of the samples were investigated under optical microscope. The microscopic images for all types of samples were compared in figure 4.16. Scanning electron microscopic images were obtained from the fractured surface to observe the fracture surface at a higher magnification.
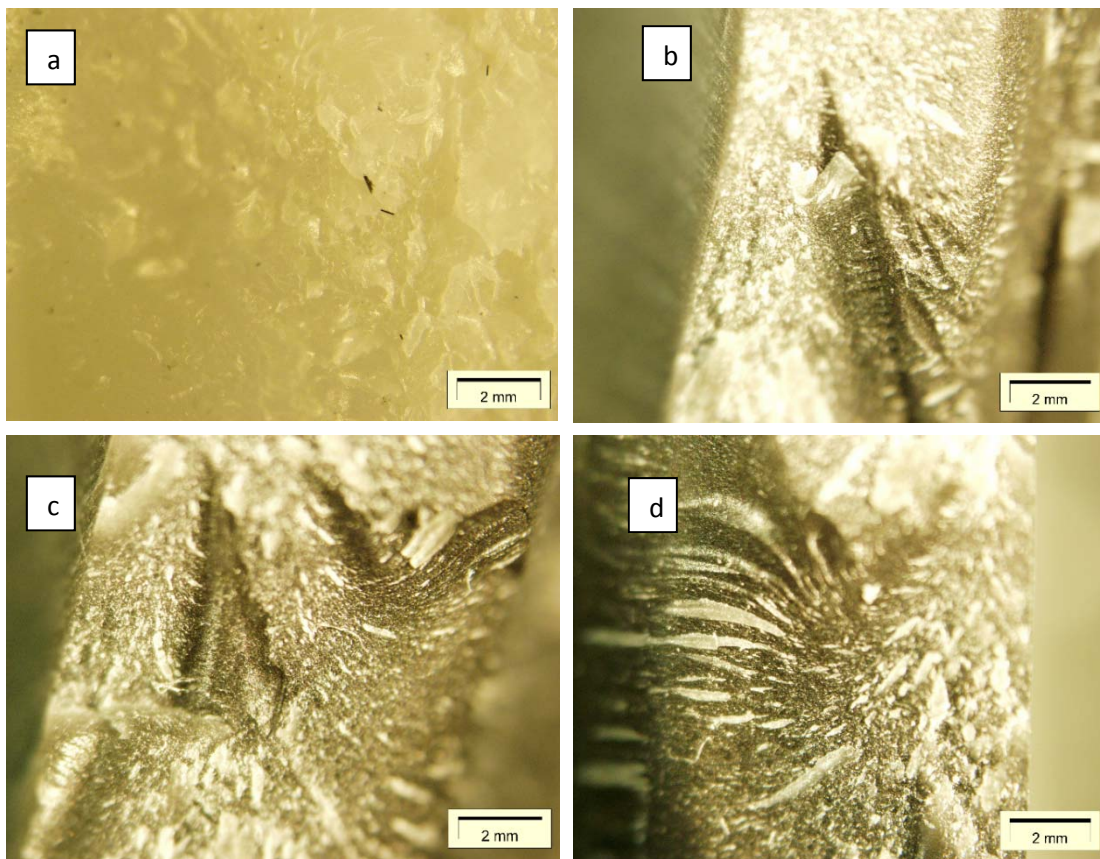
Figure 4.16 Optical microscopic images of fracture surface of fiber reinforced composites (a) control, (b) nanoclays reinforced, (c) MWCNT reinforced and (d) binary nanoparticles reinforced
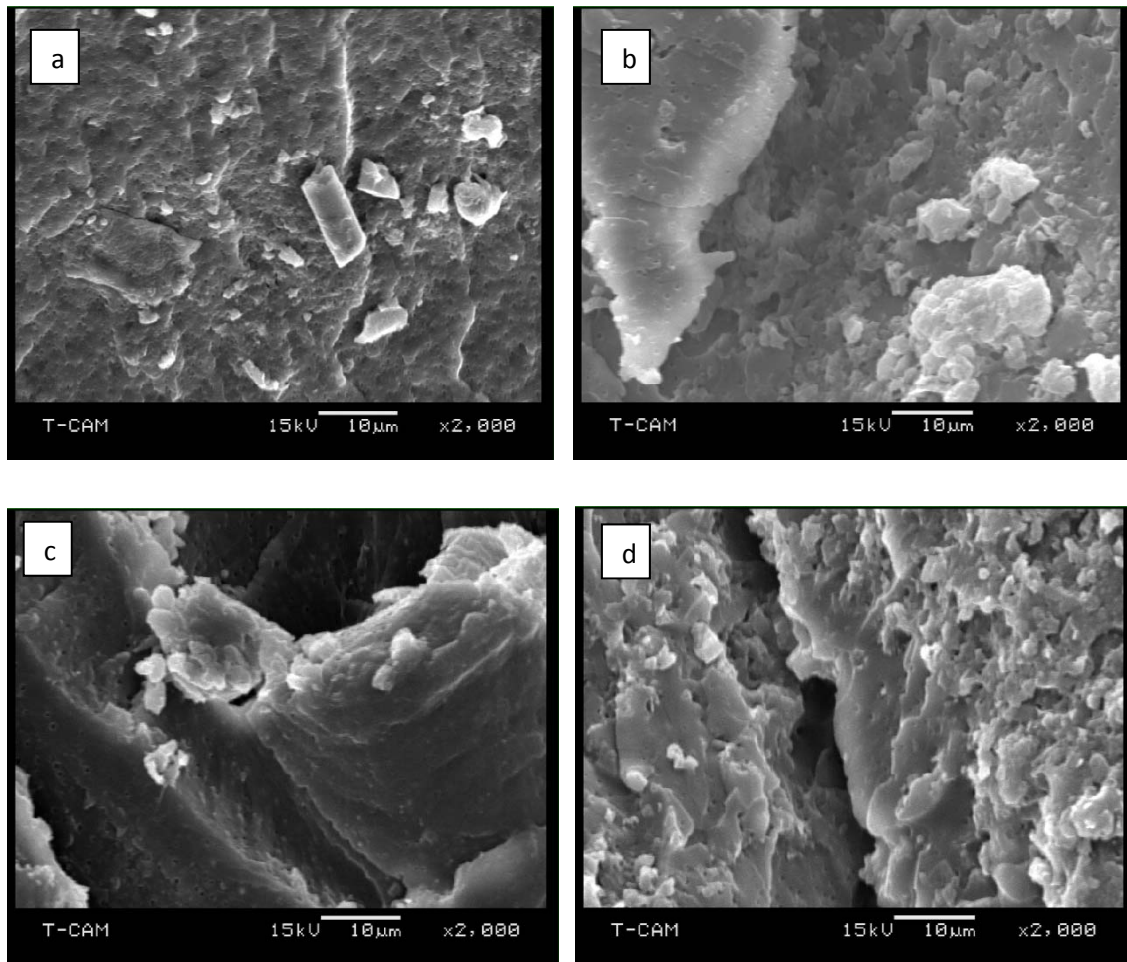
Figure 4.17 SEM images of fracture surface of nanocomposites (a) control, (b) nanoclays reinforced, (c) MWCNT reinforced and (d) binary nanoparticles reinforced.

Fracture surface of control composites were very smooth. Resin crack propagated without any hindrance as shown in figure 4.16 (a). When epoxy resin was reinforced with nanoparticles, infused nanoparticles hindered the propagation of cracks in nanocomposites. Thus, crack propagation was deflected in the nanoparticles reinforced composites. When the crack fronts faced nanoparticles they have to change the direction. Moreover, nanoparticles pullout occurred during crack propagation. Nanoparticles pullout required high energy

dissipation, which had to be supplied during testing. Nanoparticles pullout left a rough surface which is evident from the scanning electron microscopic images of samples as shown in figure 4.17. At higher magnification, micro-crack propagation were visible in figure 17 (a) for control epoxy resin. Cracks were propagated almost linearly. For nanoparticles reinforced composites, the fracture surface were rough due to nanoparticles pullout evident from figure 17 (c). For MWCNTs reinforced composites, the direction of fracture surface changed significantly. For binary nanoparticles reinforced composites, pullout of nanoparticles were much frequent than other nanoparticles reinforced composites exhibited in figure 17 (d).

4.7 Summery

Nanoparticles reinforcement enhances almost all the properties of nanocomposites evaluated from tests conducted:

➤ Flexural strength and modulus increased significantly due to nanoparticles incorporation with highest enhancement of **29%** and **44%** respectively for binary nanoparticles reinforced nanocomposites.

➤ Binary nanoparticles reinforced nanocomposites exhibited about **25%** improvement in storage modulus, loss modulus and glass transition temperature. Cross-link density appeared to be **three times** higher for binary nanoparticles reinforced nanocomposites.

➤ Coefficient of thermal expansion decreases about **30%** for binary nanoparticles incorporation before glass transition temperature.

➤ Morphological and microscopic analysis exhibit smooth fracture surface for control sample, whereas the roughness of surface increases with nanoparticles incorporation. For

binary nanoparticles reinforcement, fracture surface becomes most rough indicating

change of crack propagation direction.

5. CHAPTER V FIBER REINFORCED COMPOSITES CHARACTERIZATION

5.1 Introduction

In this research, carbon fiber reinforced epoxy composites were modified with MWCNTs, nanoclays and binary nanoparticles. All types of carbon fiber/epoxy were subjected to flexure, dynamic mechanical analysis, thermomechanical analysis, morphological and microscopic analysis to obtain mechanical, viscoelastic and thermal properties. Most of the properties such as flexure test, DMA were measured through thickness direction, whereas tensile test was conducted along the fiber axis. TMA tests were conducted through thickness and along the fiber direction. Transient data from these tests were accumulated and various properties were calculated. Properties obtained for nanoparticles modified carbon fiber/epoxy composites were compared with control carbon fiber/ epoxy composites.

5.2 Matrix digestion test

Fiber and matrix volume fraction and void content were computed in all types of samples consisting of control and nanoclay, MWCNT, hybrid nanoparticles incorporated samples. Average fiber volume fraction were 58-62% and void content were 3-5% as shown in table 5.1. Void content of control samples were lower than the nanoparticles reinforced ones. It may be attributed to the increment of resin viscosity due to the incorporation of nanoparticles. High viscosity of resin might hinder removal of gas produced at time of fabrication and facilitated entrapment of bubbles.

Table 5.1 Fiber and void volume fraction of nanophazed and control carbon fiber/epoxy composites

Types of Specimen	Control carbon fiber/epoxy composites	MWCNTs modified carbon fiber/epoxy composites	Nanoclays modified carbon fiber/epoxy composites	Binary nanoparticles modified carbon fiber/epoxy composites
Fiber Volume Fraction	58.23	59.47	59.94	60.11
Void Content	3.72	4.05	4.83	5.61

5.3 Flexural Properties of Fiber Reinforced composites

Carbon fiber reinforced composites modified with nanoparticles are subjected under three point bending load to compare the flexural properties of nanoparticles modified ones to control one. Flexural stress versus strain plots are depicted in figure 5.1. Figure 5.1 reveals the influence of nanoparticles on the flexural properties of composites. The comparison of flexural properties among the nanophazed and control composites is depicted in figure 5.2. All data accumulated is tabulated in table 5.2. Flexural strength and modulus of all the samples increased with addition of nanoparticles. The maximum enhancement was observed for binary nanoparticles modified CFRPs with an increase of 31% and 30% of flexural strength and modulus.
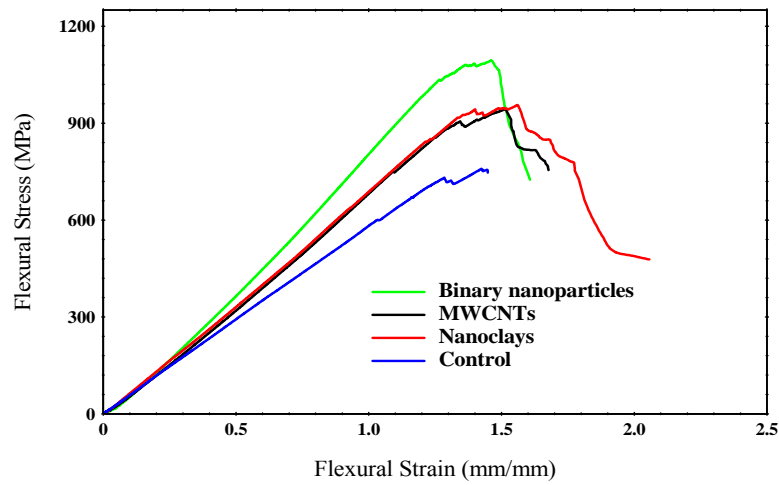
Figure 5.1 Flexural Stress versus strain response of control and nanoparticles reinforced

carbon fiber/epoxy composite samples

Table 5.2 Flexure test results of control and nanoparticles reinforced carbon fiber/epoxy

composites

Sample type	Flexural Strength	% Improved	Flexural Modulus	% Improved	Strain at maximum stress	% Improved
Control	799.63±51.83	-	56.58±2.62	-	1.53 ± 0.15	-
Nanoclay Reinforced	961.54±18.93	20	68.61±1.07	21	1.54 ± 0.05	1
MWCNT reinforced	953.71±12.32	19	64.85±2.56	15	1.54 ± 0.19	1
Binary nanoparticles reinforced	**1044.04±52.14**	**31**	**73.32±1.42**	**30**	**1.55 ± 0.22**	**1**

In section 4.2, interaction of nanoparticles with resin in the nanocomposites were discussed, where the reinforcing mechanism for epoxy resin was illustrated. Yet, in fiber reinforced composites, carbon fibers are the primary load carrying agents. Nanoparticles act as a load transfer mechanism between resin and fibers while reinforcing the resin. In bending load, the composite structure is loaded in thickness direction, in which direction the composite structures are most vulnerable. Individual plies in the composite structure are prone to separation due to shear stress on the laminate. Hence nanoparticles come into play acting as a bridge structure between the plies. Thus, when loaded these bridge structures between plies must be severed before delamination, which required more energy to break the specimen. Therefore, nanoparticles are more effective when used as a reinforcement of CFRPs as they reinforce the resin as well as act as bridge structure between individual ply.
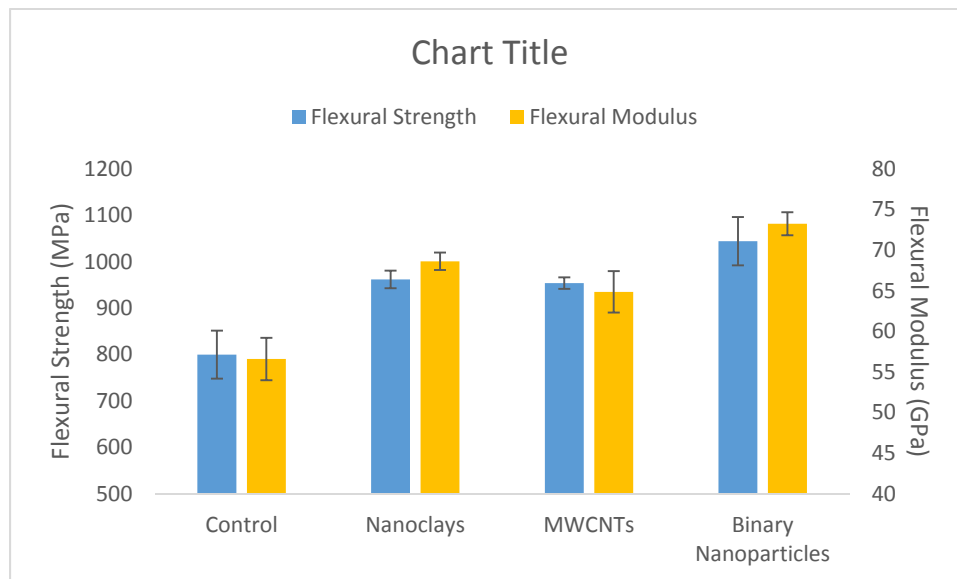
Figure 5.2 Comparison of flexural strength and modulus exhibited by nanoparticles reinforced and control carbon fiber/epoxy composites samples.

Figure 12 and 13 exhibits the morphological study on control and nanoparticles modified CFRP samples. Surface of control samples are clean and every fiber is separated as shown in SEM images. On the other hand, fiber surface of nanoparticles reinforced CFRPs have remaining resin-nanoparticles system on them. The additional adhesion between fibers and matrix can be attributed to nanoparticles. Thus, it can be concluded that nanoparticles addition is an effective way to reinforce resin as well as FRPs and binary nanoparticles are much more efficient than single nanoparticles reinforcement.

5.4 Tensile Properties

Nanoparticles reinforced carbon fiber reinforced composites were subjected under tensile load to obtain and compare the tensile properties of MWCNTs, nanoclays and binary nanoparticles reinforced FRPs with control composites.
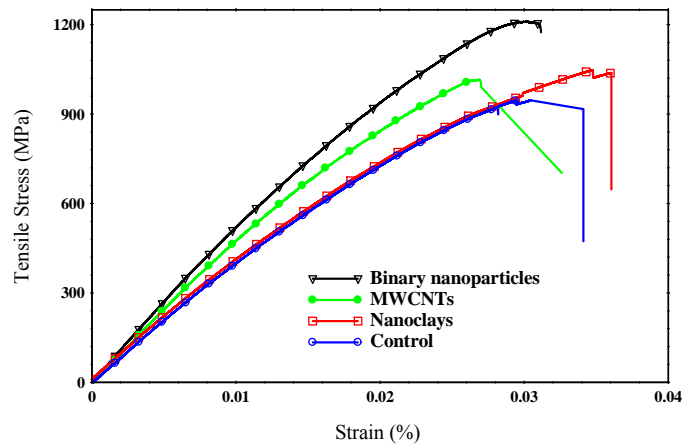
Figure 5.3 Tensile stress-strain plot exhibiting tensile properties of nanoparticles reinforced and control carbon fiber/epoxy composites
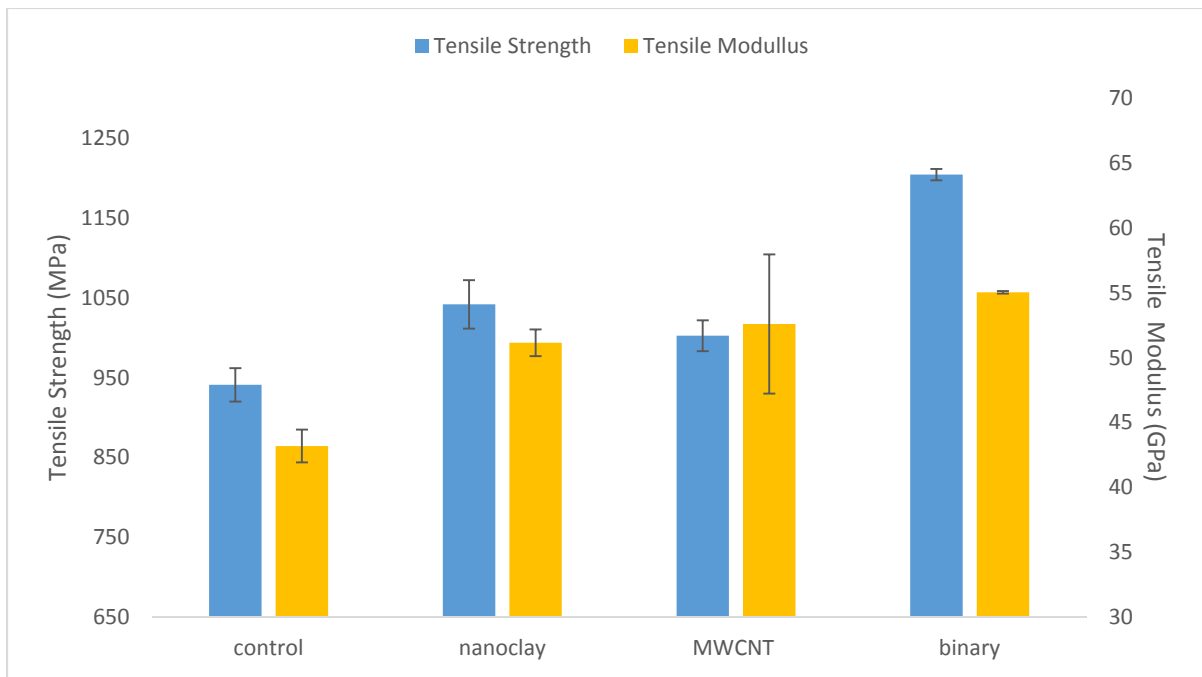
Figure 5.4 Comparison of tensile strength of nanoparticles reinforced FRPs with control

FRPs

Table 5.3 Tensile test results of control and nanoparticles reinforced carbon fiber/epoxy

composites

Sample type	Tensile Strength (MPa)	% Improved	Tensile Modulus (GPa)	% Improved	Strain at Break (%)	% Improved
Control	941±20.95	-	43.19±1.26	-	2.1 ± 0.15	-
Nanoclay Reinforced	1041.83±30.35	11	51.15±1.03	19	2.57 ± 0.05	22
MWCNT reinforced	1002.5±19.25	7	52.6±5.37	23	2.33 ± 0.31	10
Binary nanoparticles reinforced	**1204.39±7.09**	**28**	**55.04±0.1**	**27**	**3.0 ± 0.43**	**40**

Figure 5.3 exhibits tensile stress-strain plot for FRPs. From the plot, it is evident that, tensile strength and modulus enhanced for all nanoparticles reinforcement, although for binary nanoparticles the increment was highest. Figure 5.4 and table 5.3 shows the comparison of tensile strength, and modulus for all nanoparticles reinforced composites. Binary nanoparticles reinforced FRPs exhibits 28%, 27% and 40% improvement in tensile strength, strain and modulus respectively. All data related to the experiment are shown in table 5.3. Nanoparticles reinforcement of fiber reinforced composites results in multiscale reinforcement. Nanoparticles function as a bridge structure between each lamina. At time of delamination they try to hold the laminates in place and arrest delamination. Moreover, matrix cracking is a common phenomenon in fracture due to tensile loading. In fiber reinforced composites, matrix reinforcement through chemical reaction of resin and nanoparticles takes place according to the reaction mechanism described in section 4.2. Crack propagation in matrix is restricted due to presence of nanoparticles. When crack propagates, nanoparticles are pulled off from the matrix. Energy dissipation mechanism occurs while pulling the nanoparticles from the matrix and form void. Thus, higher load is required for failure in case of nanoparticles reinforced composites. Figure 5.10 and 5.11 exhibits the optical microscopic images of the fracture surface of samples under tensile loading. The fracture surface of control composites are much smooth with less delamination. Yet, the fracture surface of nanophazed composites FRPs is rough and broken sharp edged fibers are pulled out from the fracture surface due to loading. It is due to superior adhesion between fiber and matrix resulting in successful energy transfer from matrix to fiber achieved through nanoparticles reinforcements. In binary nanoparticles reinforced composite samples,

more numbers of nanoparticles are pulled off from the matrix and also the resin-nanoparticles matrix are bonded chemically to a more rigid network. Therefore, binary nanoparticles reinforcement is more effective than other reinforcements.

5.5 DMA of FRPs

Nanophazed and control carbon fiber/epoxy composites were subjected under dynamic mechanical analysis to obtain viscoelastic properties. Transient data obtained from this experiment were accumulated and storage modulus, loss modulus, tan-delta as a function of temperature were plotted in figure 5.5- 5.8. Peak storage modulus, loss modulus and tan-delta values as well as glass transition temperature were tabulated in table 5.4. The standard deviation of all peak value were trivial.
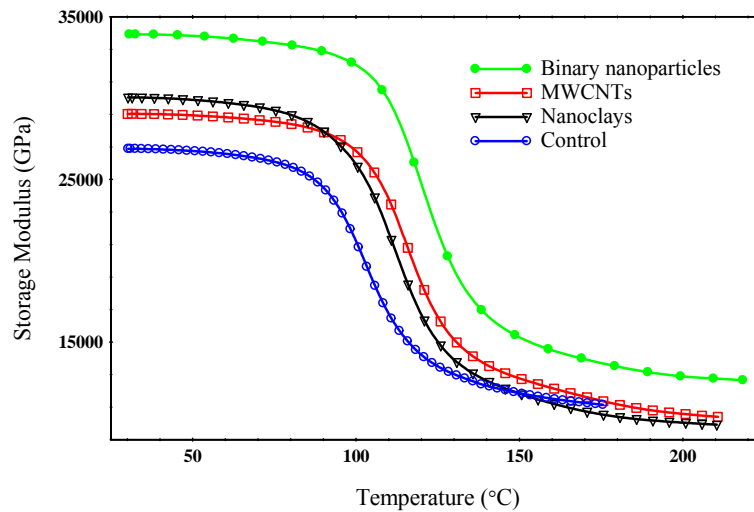
Figure 5.5 Storage modulus of nanoparticles reinforced and control fiber reinforced composites

Table 5.4 DMA results of control and nanoparticles reinforced carbon fiber/epoxy composites

Sample Type	Storage modulus (MPa)	% Change	Peak loss modulus (MPa)	% Change	Glass Transition Temperature	% Change	Peak tan-delta $\times 10^{-2}$	% Change
Control epoxy resin	25460.25 ± 1302.86	-	1725.95 ± 60.59	-	107.67 ± 1.55	-	9.92 ± 0.27	-
Nanoclays reinforced	30105.3 ± 78.63	18	2374.74 ± 25.13	38	120.36 ± 0.76	12	10.89 ± 0.89	10
MWCNTs reinforced	29020.5 ± 757.51	14	2215.32 ± 116.77	30	116.31 ± 2.36	8	11.34 ± 0.95	21
Binary nanoparticles reinforced	34311 ± 737.97	40	2458.83 ± 63.04	44	127.11 ± 3.14	19	12.26 ± 0.08	29

5.5.1 Storage modulus

Storage modulus of all sample as a function of temperature is depicted in figure 5.5. Moreover, the peak values of storage modulus for samples were compared in figure 5.7. From figure 5.7, it is evident that binary nanoparticles reinforced carbon fiber/epoxy composites possess much higher storage modulus and glass transition temperature than control composites. Moreover, nanoclays reinforced composites had higher storage modulus, yet lower glass transition temperature. On the contrary, MWCNTs reinforced composites exhibited lower storage modulus, yet high glass transition temperature. Therefore, in binary nanoparticles reinforced composites, MWCNTs tend to increase the glass transition

temperature along with nanoclays reinforcing the resin mechanically. The mechanism of nanoparticles reinforcing resin is described in section 4.2 and its influence on viscoelastic properties were illustrated in section 4.4.

5.5.2 Loss Modulus

Loss modulus of control and nanophazed carbon fiber/epoxy composites are presented in Figure 5.6. Loss modulus for nanoparticles reinforced carbon fiber/epoxy composites is much higher than the control composites. Binary nanoparticles possess highest loss modulus, thus highest amount of energy is dissipated while three point bending load is applied. When the load is applied, the nanoparticles try to hold the laminae in place, so more amount of energy is required to deform the samples. Thus, nanoparticles reinforced composites required higher load and loss modulus increased for nanophazed composites.
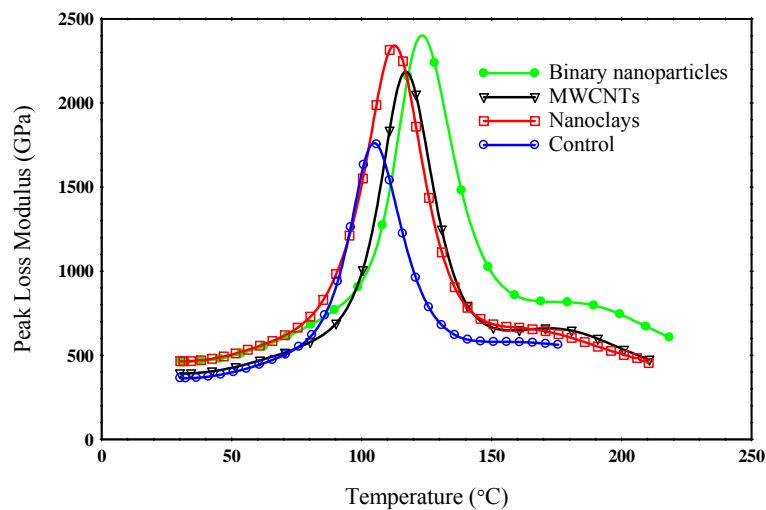
Figure 5.6 Loss modulus of nanoparticles and control fiber reinforced composites
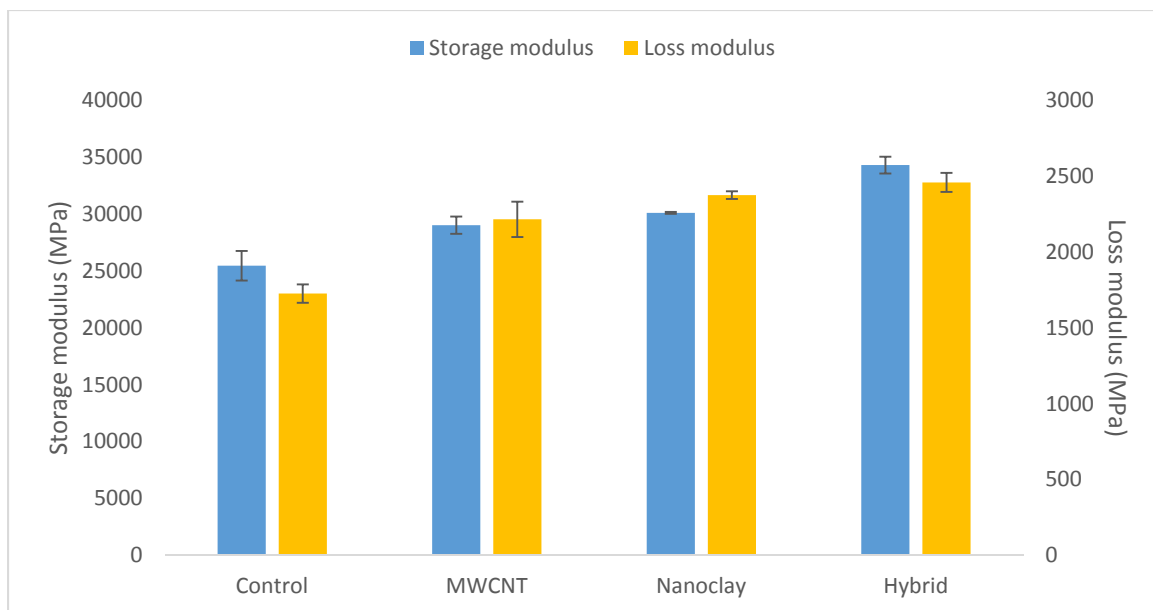
Figure 5.7 Comparison of storage and loss modulus of nanoparticles reinforced carbon fiber/epoxy with control ones

5.5.3 Tan-delta

Peak values of tan-delta versus temperature plot indicates the damping properties of the composites. Damping properties of nanophazed composites are much higher than control composites. Binary nanoparticles increase 29% of damping properties of carbon fiber/epoxy composites. Also glass transition temperature obtained from tan-delta plot exhibits similar behavior as nanocomposites. Nanoclays, MWCNTs and binary nanoparticles increases the glass transition temperature about 12%, 8% and 19% respectively. Improvement for carbon fiber/epoxy composites while incorporated with nanoparticles are lower than the improvement of nanocomposites in case of nanoparticles infusion.
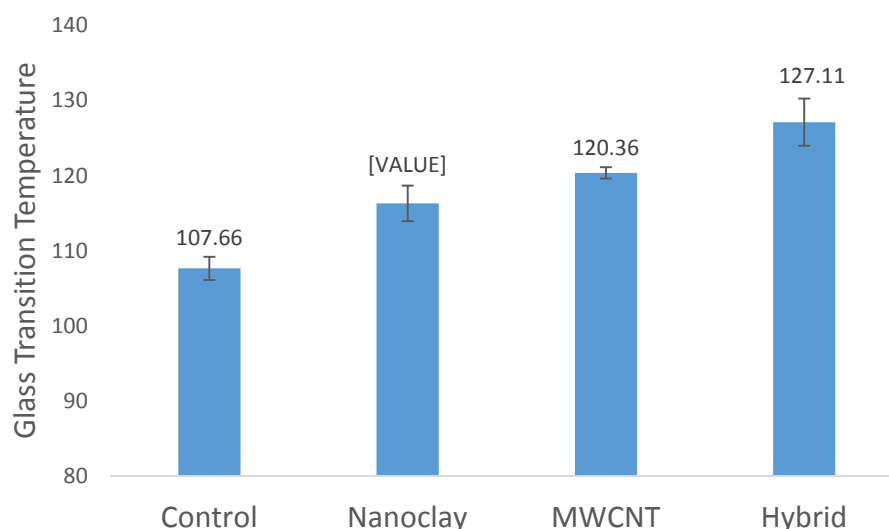
Figure 5.8 Glass transition temperature obtained from tan-delta plot of carbon fiber /epoxy

composites.

5.6 Thermo-mechanical analysis of FRPs

Thermo-mechanical analysis of control and nanoparticles reinforced carbon fiber/epoxy composites reveals distinct behavior while performed in different direction. Coefficient of thermal expansion for carbon fiber is negative, thus carbon fiber contracts when temperature increases. On the contrary, epoxy SC-15 resin has a positive CTE. Therefore, carbon fiber reinforced epoxy composites were subjected under thermomechanical analysis in both direction-along fiber axis and through thickness direction. Coefficient of thermal expansion were calculated from the dimension change versus temperature plot obtained in both direction. Dimension change versus temperature plots through thickness direction were similar to the plots obtained for TMA of nanocomposites. Thus, CTE values were obtained

from the slope of the plots before and after glass transition temperature. Glass transition temperature was obtained from nadir of the plots. CTE values and glass transition temperature for nanophazed and control composites are depicted in figure 5.8 and table 5.5. It is evident that, the CTE of binary nanoparticles are lowest among all samples before and after glass transition temperature. When CTE is measured through thickness direction, it depends on resin. As described in section 4.5, nanoparticles tend to decrease CTE of nanocomposites. Thus, in control composites when temperature increases, resin starts to transform rubbery from glassy structures and each lamina becomes separated. In contrary, for nanoparticles modified carbon fiber reinforced composites, nanoparticles reinforce the matrix structure as well as act as bridging structures to laminates. Thus nanoparticles reinforced carbon fiber/epoxy composites expands less than control composites. For binary nanoparticles, nanoclays reinforce the resin being exfoliated in them whereas, MWCNTs act as bridging structure between laminae.
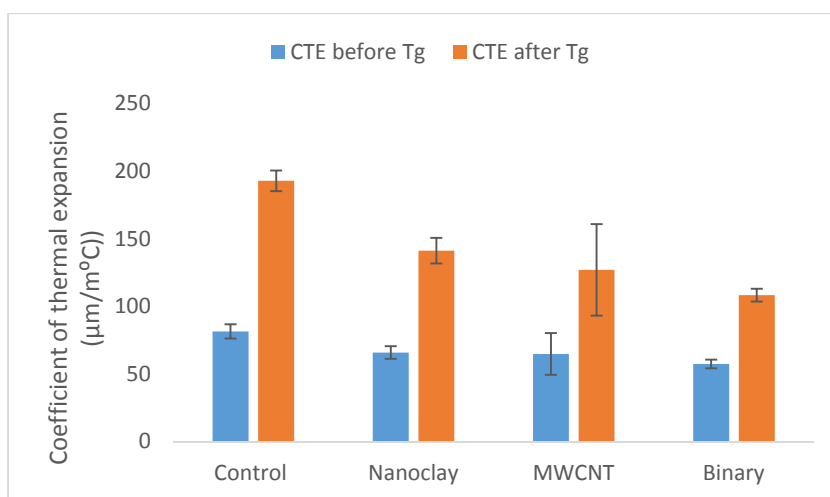
Figure 5.9 Coefficients of thermal expansion before and after glass transition temperature for composites measured through thickness
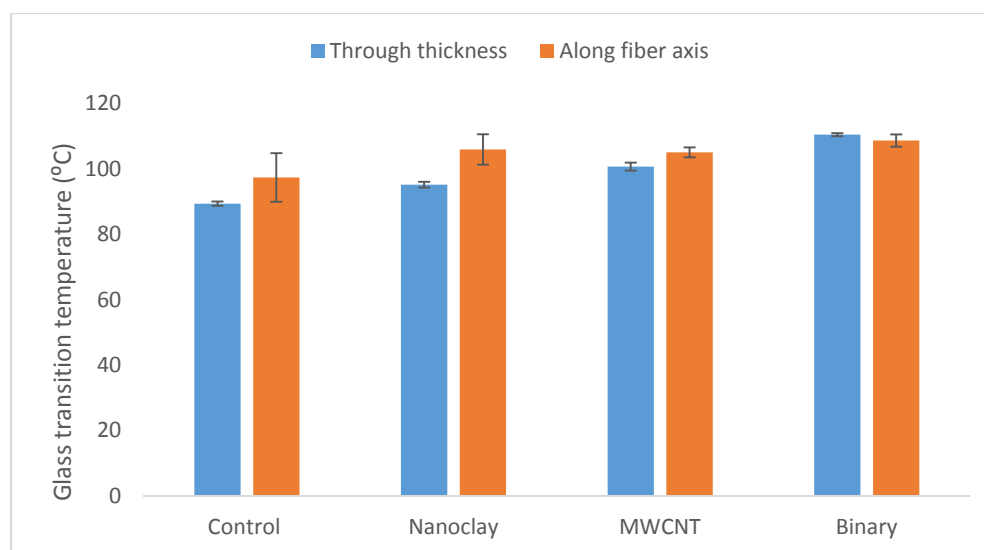
Figure 5.10 Glass transition temperature of nanocomposites from TMA for composites measured along fiber axis and through thickness

Table 5.5 TMA results for carbon fiber/epoxy composites through thickness

Sample Type	CTE before T_g	% Improvement	CTE after T_g	% Improvement	T_g	% Improvement
Control	81.38±5.28	-	192.78±7.61	-	89.33±0.67	-
Nanoclay reinforced	65.78±4.67	20	141.07±9.49	26	95.13±0.88	7
MWCNT reinforced	64.71±15.42	21	126.89±33.86	34	100.67±1.21	13
Binary nanoparticle	57.3±3.18	30	108.2±4.71	44	110.42±0.45	24

Along fiber direction, slope of dimension change versus temperature yields opposite direction. Thus, CTE values for composites become negative before and after glass transition temperature. Moreover, the CTE values are very near to zero. CTE values for fibers are negative and trifle compared to resin

Table 5.6 TMA results for carbon fiber/epoxy composites along fiber direction

Sample Type	CTE before T_g	CTE after T_g	T_g
Control	-1.82 ± 2.58	-4.66 ± 1.73	97.34±7.45
Nanoclay reinforced	-2.34 ± 2.57	-2.08 ± 1.46	105.89±4.66
MWCNT reinforced	-3.96 ± 8.069	-3.58 ± 2.77	105.01±1.51
Binary nanoparticle	-0.062 ±.077	-2.58 ± 2.21	108.61±1.87

. Along fiber direction, CTE values are very similar to fiber CTE as shown in table 5.6. For nanoparticles reinforced composites, no significant change in CTE was exhibited as nanoparticles generally influence resin control properties. Therefore, binary nanoparticles reinforcement significantly improved CTE through thickness, whereas, no substantial influence was observed on CTE along fiber axis.

5.7 Microscopic analysis of carbon fiber/epoxy composites

For composite structures, numerous fracture modes play significant role; such as interlaminar failure, matrix cracking, fiber breaking, matrix-fiber deboning and fiber pullout. The primary ground of damage in the laminates under tensile test is matrix cracking and fiber pullout (Prasad, Venkatesha, & Jayaraju, 2011). Delamination is also common phenomenon in case of fracture. Delamination may occur due to any three type of loading: mode I-Tensile Mode, Mode II-Sliding mode, Mode III- tearing mode or combination of these modes. To observe the mode of failure, the specimens were observed under optical microscope and the images are presented in figure 5.11 and 5.12. Figure 5.11 shows the front view of the samples failed during tensile test. Figure 5.12 portrays the images from the optical microscope of the lateral portion of the samples. The image of binary nanoparticles reinforced sample in figure 5.12

depicts about all modes of failure such as, interlaminar failure of mode I and II, matrix cracking, fiber pullout and fiber breakage. For nanoclay modified samples, fiber breakage and matrix cracking were observed along with partial delamination. For, MWCNT modified samples, slight fiber breakage and matrix cracking were found with minor delamination of the fibers. Yet, control samples portrays typical fiber pullout and matrix cracking. Matrix cracking took place without any hindrance in control samples and fibers were pulled out. Thus, much less energy were required for the failure of control samples.
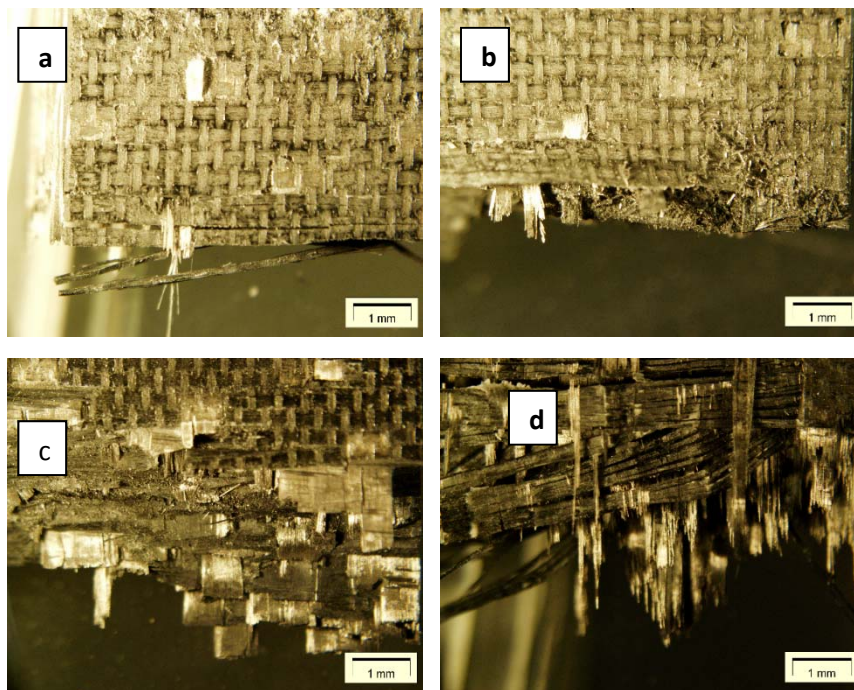
Figure 5.11 Optical microscopic images of front views of fracture surface of FRPs (a) control, (b) nanoclays reinforced, (c) MWCNT reinforced and (d) binary nanoparticles reinforced.

In case of binary nanoparticles reinforced composites, resin was reinforced with nanoparticles. Thus matrix cracking faced a lot of hindrance due to presence of nanoparticles. Meanwhile other modes of failure occurred. All these failure modes required much higher energy than matrix cracking and fiber pullout. Therefore, highest energy was required to fail while the test were conducted for binary nanoparticles reinforced composites.
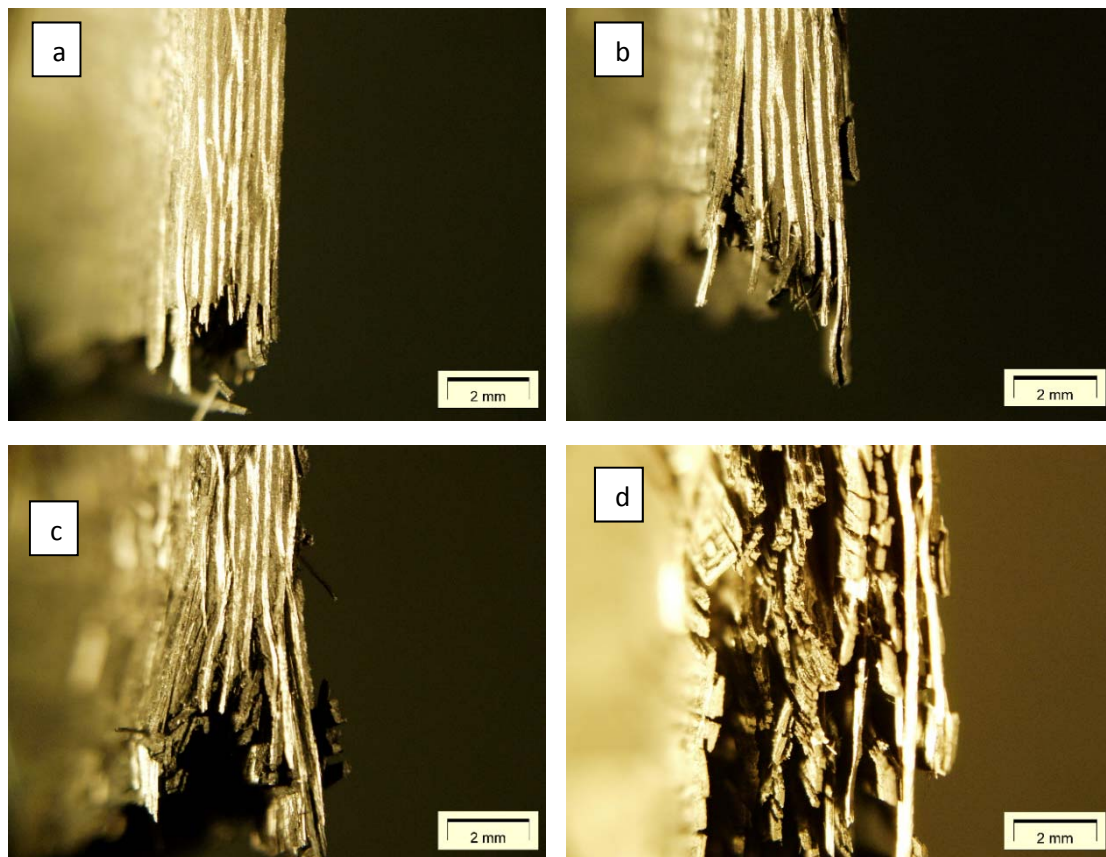
Figure 5.12 Optical microscopic images of side views of fracture surface of fiber reinforced composites (a) control, (b) nanoclays reinforced, (c) MWCNT reinforced and (d) binary nanoparticles reinforced

Fractured surface of different specimen is analyzed through scanning electron microscope. The surface was sputtered with gold and placed under electron beam at 15kV. At first,

fracture surface of all the specimen was observed at 1000x magnification level. Figure 5.13 depicts the images obtained for nanophazed and control carbon fiber/epoxy composite on delaminated fracture surface of tensile samples. Likewise, 1500x magnification were employed to get images from the fracture surface of flexure test samples as shown in figure 5.14. Nanophazed and control samples in both case resembled similar appearance. In case of control samples in figure 5.13 (a) and 5.14(a), fibers from the fractured surface were completely pulled out for the matrix and the fibers were completely separated as well as severe matrix cracking took place.
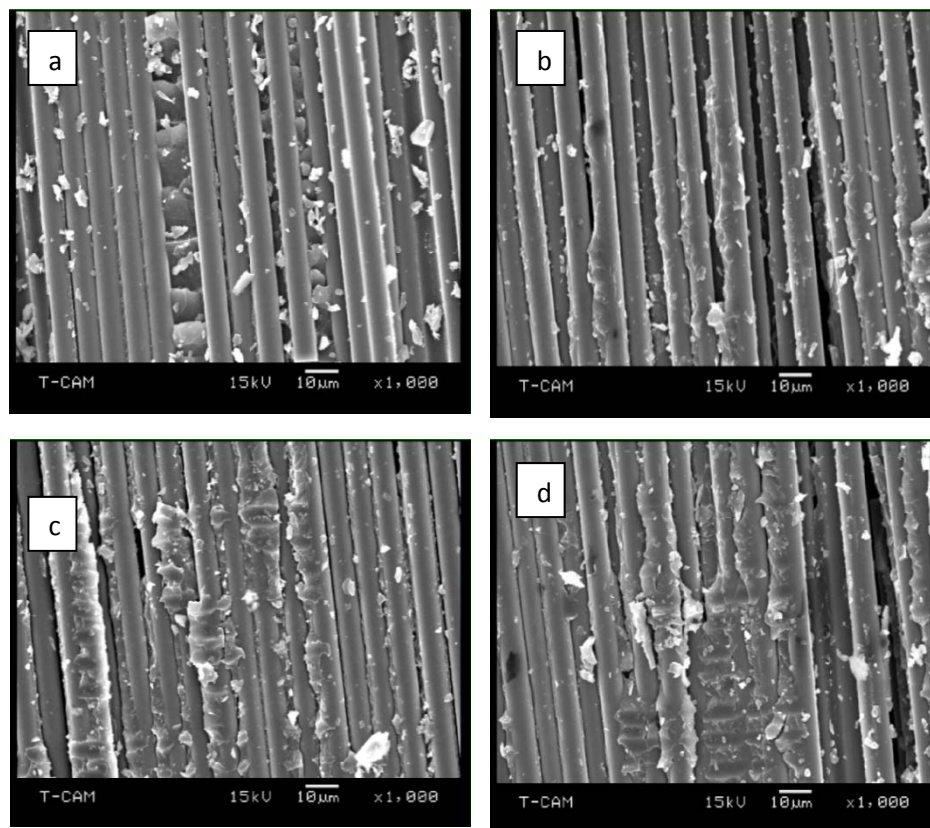
Figure 5.13 SEM images of fracture surface of fiber reinforced composites at X1000 zoom

level (a) control, (b) with nanoclays, (c) with MWCNT and (d) with binary nanoparticles.
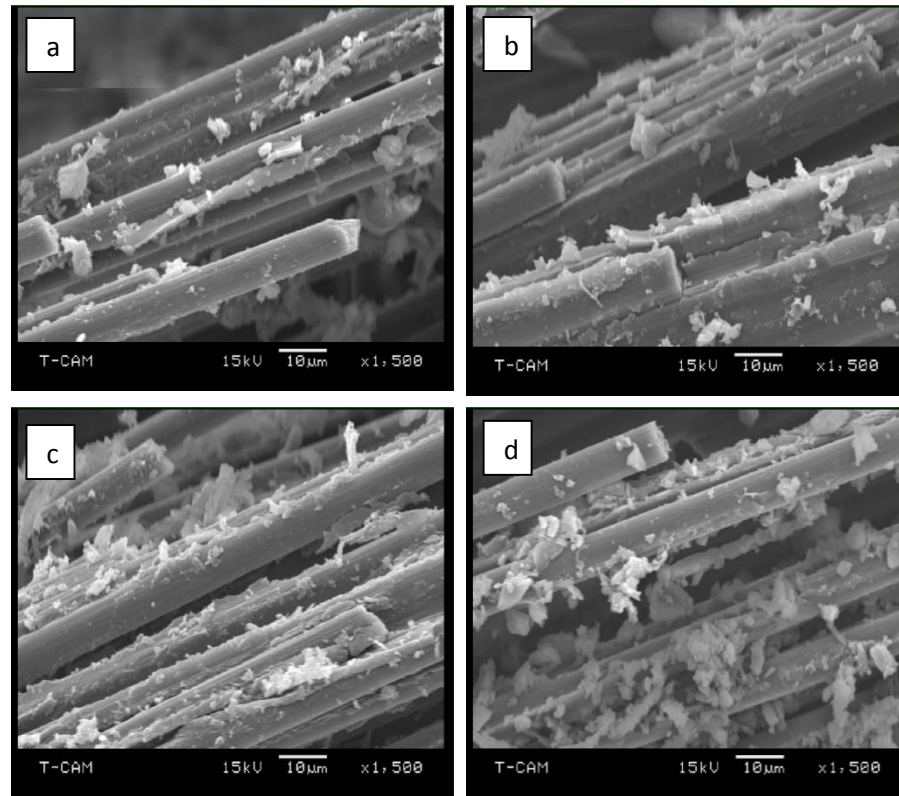
Figure 5.14 SEM images of fracture surface of fiber reinforced composites at X1500 zoom

level (a) control, (b) nanoclays reinforced, (c) MWCNT reinforced and (d) binary

nanoparticles reinforced

On the contrary, microscopic images for MWCNT and hybrid nanoparticles modified

composite samples shown partial pull out of fibers from the matrix. Although some of the

fibers were separated completely, most of the fibers were attached with others which might

be attributed to additional delamination mechanism presented by MWCNTs in nanophazed

samples (Kostopoulos et al., 2010). Nanotubes, dispersed in resin acts as a bridging structure

between the laminas. Hence, at the time of delamination, the bonding between resin and

nanotubes as well as bonding between resin and carbon fibers have to be severed. This incident results in absorbing more energy than the control laminates as well as arresting the development of cracks due to fracture and damaging mechanism. On the other hand, nanoclays are layered structures, when dispersed and exfoliated in resin, serves as reinforcement to the resin. Thus, it might check the progress of matrix cracking to reduce the damage in the composite structures. Now, binary nanoparticles modified samples have both MWCNTs and nanoclays as reinforcement. Hence, MWCNT might act as a bridge structure between the laminae and nanoclays reinforced the matrix materials hereby diminishing delamination as well as matrix cracking of the samples.

5.8 Fatigue Characterization of Nanoclay Reinforced carbon fiber/epoxy composites

Static tensile test was performed to obtain the ultimate strength and modulus of nanoclay reinforced and control carbon fiber reinforced composites. Rectangular coupon from each type of samples was subjected to tensile stress. Transient data consisting load and displacement were accumulated. Stress and strain values were computed and stress-strain plot was drawn. Tensile stress-strain curve are non-linear due to its dependence on polymer matrix (Khan et al., 2010). No yield strength was observed, yet failure stress increased with the nanoclay content increment. Figure 5.17 depicts the stress versus strain curves for all samples. It can be observed that the ultimate strength of 1 and 2 wt. % nanoclay modified CFRPs are much higher compared to control samples. Although 2 wt. % nanoclay modification results in higher ultimate strength, 1 wt. % nanoclay modified ones show higher tensile modulus. Tensile strength and modulus for all samples are tabulated in table 1.

Tensile strength and modulus enhanced with nanoclay percentage revealing its relation with matrix property. Figure 5.13 and 5.14 exhibit the fracture surface of control and nanophazed specimen depicting sharp contrast. In the case of control samples, fibers from the fractured surface were completely pulled out for the matrix and the fibers were completely separated. There was severe matrix cracking due to the impact. Although some of the fibers were separated completely due to the high stress, most of the fibers were attached with others. Nanoclays, dispersed in resin act as bridging structures at microscopic level between the laminae. Hence, at the time of delamination, the bonding between resin and nanoparticles as well as bonding between resin and carbon fibers has to be severed. This incident results in more energy absorption than in case of control laminates. They also effect in arresting the development of cracks due to fracture. Moreover, nanoclays are layered structures, when dispersed and exfoliated in resin, serves as reinforcement to the resin. They develop strong interfacial bonds between matrix and fibers. Thus, they check the progress of matrix cracking to reduce the damage in the composite structures.
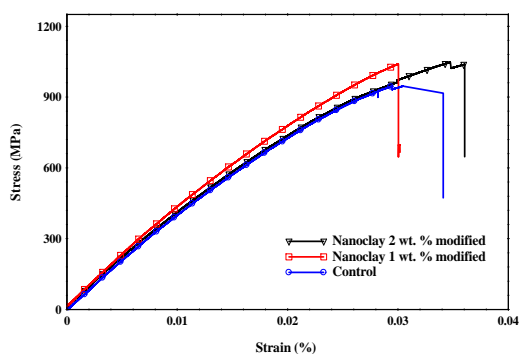
Figure 5.15 Stress vs. strain behavior for static tensile test for carbon fiber reinforced epoxy composites

Table 5.7 Tensile Strength and modulus of control and nanoclay reinforced CFRPs

Sample	Control	1 wt. % nanoclay modified	2 wt. % nanoclay modified
Tensile Strength (MPa)	941±20.95	1018.667±67.12	1041.833±30.34
Tensile modulus (GPa)	43.19±2.56	51.15± 3.79	43.94±2.84

Fatigue characterization was carried out at three stress level 90%, 80% and 70% of ultimate tensile strength. Three coupons of each type of samples were tested for each stress level. Cyclic stress versus lifetime curves are depicted in Figure 5.18 and a log-normal fitting parameters are presented in table 5.8. From figure 5.18, it can be observed that, nanoclay modification of carbon fiber/epoxy composite samples shifts the curve towards higher life cycle for same stress amplitude with slight change in the slope of the curves. For low stress or high cycle regime, the nanoparticles seems to be more effective than the low cycle high stress amplitude regime. This phenomena may be explained through microstructure analysis. For, low stress amplitude fatigue, nanoparticles can arrest the fatigue crack growth as mentioned above, but for high stress, initiation of multiple crack fronts occurs at the same time. Higher load causes higher strain energy density. Moreover, the fatigue crack grows at a faster rate. High strain intensity results in stress concentration in matrix. Therefore, nanoparticles cannot play an important role to hinder the crack propagation or multiple crack initiation. Thus, nanoparticles can enhance the fatigue strength at lower stress more than higher stress.

Fracture surface of control and nanophazed FRPs are investigated under optical microscope. Coupons failed due to matrix failure, fiber breakage and delamination of plies. Matrix

cracking is critical reason of failure for control samples. In case of control samples crack initiation in matrix resulted in ultimate failure rapidly. For nanophazed samples, crack growth propagates at a much slower rate. Nanoparticles arrested the crack propagation and transferred load successfully from matrix to fibers. This phenomena reinforced matrix while fibers breakage and delamination of plies occurred. Thus, in case of nanoclays reinforced composites all fracture mechanism remains present.
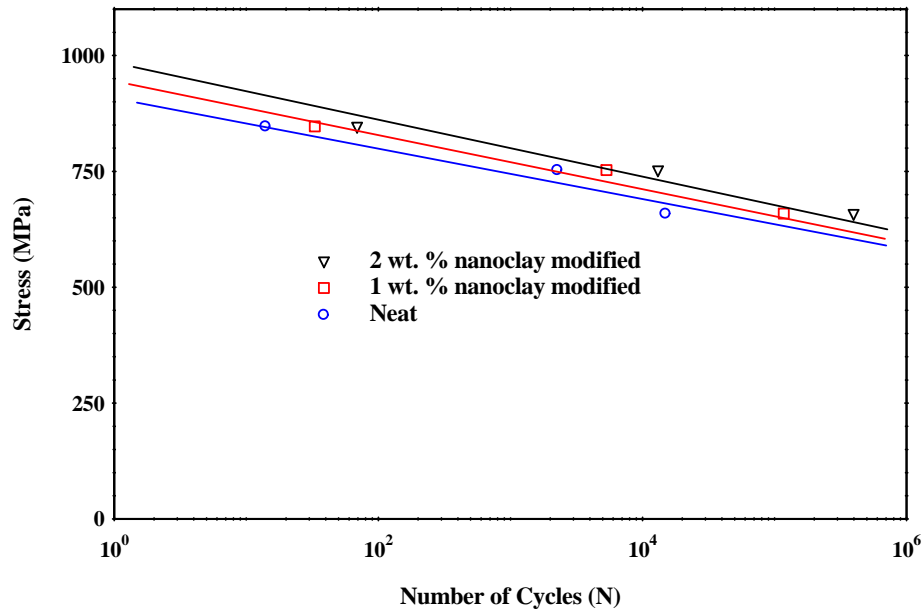
Figure 5.16 Cyclic stress verses logarithmic scale of cycles to failure (S–N curves) for neat and 1.0 wt. % CNF reinforced epoxy

Table 5.8 Fatigue mean fit parameters (log values given for A and B)

Material	A	B	Estimated normal population varience, σ^2
Control	15.17	-0.016	0.1808
1 wt. % nanoclay	17.76	-0.019	0.092508
2 wt. % nanoclay	20.78	-0.022	0.117554

5.9 Summery

Nanoparticles reinforcement enhances almost all the properties of CFRPs evaluated from tests conducted. Binary nanoparticles exhibited best properties among the nanoparticles reinforced composites:

> Flexural strength and modulus increased about **30%** and **31%** respectively for binary nanoparticles reinforced nanocomposites.

> Tensile strength, modulus and strain increased about **28%**, **27%** and **40%** for binary nanoparticles incorporation.

> Binary nanoparticles reinforced nanocomposites exhibited about **40%, 44% and 19%** improvement in storage modulus, loss modulus and glass transition temperature.

> Coefficient of thermal expansion differs substantially when measured along fiber axis and through thickness direction.

➢ Coefficient of thermal expansion decreases about **30% and 44%** respectively for binary nanoparticles incorporation before and after glass transition temperature when measured through thickness. Along fiber direction nanoparticles incorporation does not influence the CTE significantly.

➢ Morphological and microscopic analyses exhibit higher interfacial adhesion of resin and fibers for nanoparticles incorporation. For binary nanoparticles, interfacial adhesion results in much more load carrying capability for composites compared to other nanophazed or control composites.

Fatigue performance of nanoclay reinforced composites were better than the control carbon fiber/epoxy composites. Results from fatigue test revealed the followings

➢ Static tensile tests exhibit highest tensile strength for 2 wt. % nanoclay reinforced samples and highest tensile modulus for 1 wt. % nanoclay reinforced samples.

➢ Tensile fatigue test reveals highest life cycle for 2 wt. % nanoclays reinforced composites under same load.

➢ Nanoclay modification of carbon fiber/epoxy composite samples shifts the curve towards higher life cycle for same stress amplitude with slight change in the slope of the curves.

➢ For low stress or high cycle regime, the nanoparticles seems to be more effective than the low cycle high stress amplitude regime.

6. CHAPTER VI CONCLUSION AND FUTURE SCOPES

In this research, epoxy SC-15 resin and carbon fiber /epoxy composites were reinforced with nanoclays, MWCNTs and binary nanoparticles. 2 wt. % of nanoclays reinforcement results in best properties among nanoclays reinforced composites. Likewise, 0.3 wt. % of MWCNTs reinforcement results in best properties among MWCNTs reinforced composites. Due to hazardous nature of MWCNTS, combination of 2 wt. % nanoclays and only 0.1 wt. % of MWCNTs were infused with resin. Composites were fabricated and subjected to various tests to obtain mechanical, thermal, viscoelastic and morphological properties. From the test results it can be concluded that:

➢ Different dispersion techniques were utilized to ensure uniform dispersion of nanoclays, MWCNTs and binary nanoparticles in resin. For MWCNTs ultrasonication and three roll shear mixture techniques were used. For nanoclays magnetic stirring was employed along with ultrasonication. For binary nanoparticles, combination of all three were used.

➢ Nanoparticles reinforcement enhances almost all the properties of nanocomposites evaluated from flexure, DMA, TMA and morphological tests conducted. Binary nanoparticles reinforced nanocomposites exhibited best properties with an increase of about 25-40% in almost all properties revealed from the tests conducted.

➢ Flexure, tensile, DMA, TMA reveals that nanoparticles reinforcement enhances the properties of CFRPs. Binary nanoparticles exhibited best properties among the nanoparticles reinforced composites. In almost all tests binary nanoparticles reinforced

carbon fiber/epoxy composites exhibited about 20-30% improvement. TMA revealed no significant influence of nanoparticles on CTE along fiber axis.

➢ 2 wt. % loading of nanoclays exhibits highest life cycle in fatigue testing of nanoclays reinforced composite samples. Moreover, nanoparticles reinforcement was more efficient for low stress high cycle regime compared to high cycle low stress regime.

6.1 Future Scope

In future, there are numerous scopes to work on:

➢ Fatigue tests for MWCNTs and binary nanoparticles reinforced composites can be conducted.

➢ Environmental degradation of properties of binary nanoparticles reinforced composites can be investigated.

➢ Various combination of nanoparticles can be tried to reinforce composites to check their compatibility with epoxy resin together.

7. CHAPTER VII WORK CITED

Ahmad, K. Z. K., Ahmad, S. H., Tarawneh, M. a., & Apte, P. R. (2012). Evaluation of Mechanical Properties of Epoxy/Nanoclay/Multi-Walled Carbon Nanotube

Nanocomposites using Taguchi Method. Procedia Chemistry, 4, 80–86. doi:10.1016/j.proche.2012.06.012

Alamri, H., & Low, I. M. (2013). Effect of water absorption on the mechanical properties of nanoclay filled recycled cellulose fibre reinforced epoxy hybrid nanocomposites. Composites Part A: Applied Science and Manufacturing, 44, 23–31. doi:10.1016/j.compositesa.2012.08.026

Alexandre, M., & Dubois, P. (2000). Polymer-layered silicate nanocomposites : preparation, properties and uses of a new class of materials. Materials Science and Engineering, 28(March), 1–63.

Avila, A. F., Soares, M. I., & Silva Neto, A. (2007). A study on nanostructured laminated plates behavior under low-velocity impact loadings. International Journal of Impact Engineering, 34(1), 28–41. doi:10.1016/j.ijimpeng.2006.06.009

Ayatollahi, M. R. (2011). ch ive, c(10), 835–843.

Azeez, A. A., Rhee, K. Y., Park, S. J., & Hui, D. (2013). Epoxy clay nanocomposites – processing, properties and applications: A review. Composites Part B: Engineering, 45(1), 308–320. doi:10.1016/j.compositesb.2012.04.012

Böger, L., Sumfleth, J., Hedemann, H., & Schulte, K. (2010). Improvement of fatigue life by incorporation of nanoparticles in glass fibre reinforced epoxy. Composites Part A: Applied Science and Manufacturing, 41(10), 1419–1424. doi:10.1016/j.compositesa.2010.06.002

Bortz, D. R., Merino, C., & Martin-Gullon, I. (2011). Carbon nanofibers enhance the fracture toughness and fatigue performance of a structural epoxy system. Composites Science and Technology, 71(1), 31–38. doi:10.1016/j.compscitech.2010.09.015

Bortz, D. R., Merino, C., & Martin-Gullon, I. (2012). Augmented fatigue performance and constant life diagrams of hierarchical carbon fiber/nanofiber epoxy composites. Composites Science and Technology, 72(3), 446–452. doi:10.1016/j.compscitech.2011.12.006

Chan, M., Lau, K., Wong, T., Ho, M., & Hui, D. (2011). Mechanism of reinforcement in a nanoclay/polymer composite. Composites Part B: Engineering, 42(6), 1708–1712. doi:10.1016/j.compositesb.2011.03.011

Chen, Q., Zhao, Y., Zhou, Z., Rahman, A., Wu, X.-F., Wu, W., … Fong, H. (2013). Fabrication and mechanical properties of hybrid multi-scale epoxy composites reinforced with conventional carbon fiber fabrics surface-attached with electrospun carbon nanofiber mats. Composites Part B: Engineering, 44(1), 1–7. doi:10.1016/j.compositesb.2012.09.005

Choi, B. J., Zhang, Y., Science, A. M., & Llc, S. C. (2014). Properties and Applications of Single- , Double- and Multi-Walled Carbon Nanotubes, 1–5.

Choi, S., & Kim, J. (2013). Thermal conductivity of epoxy composites with a binary-particle system of aluminum oxide and aluminum nitride fillers. Composites Part B: Engineering, 51, 140–147. doi:10.1016/j.compositesb.2013.03.002

Choudhary, V., & Gupta, A. (2011). Polymer/Carbon Nanotube Nanocomposites. In S. Yellampalli (Ed.), Carbon Nanotubes - Polymer Nanocomposites. doi:10.5772/18423

Chowdhury, F. H., Hosur, M. V., & Jeelani, S. (2006). Studies on the flexural and thermomechanical properties of woven carbon/nanoclay-epoxy laminates. Materials Science and Engineering: A, 421(1-2), 298–306. doi:10.1016/j.msea.2006.01.074

Cooper, C. a., Young, R. J., & Halsall, M. (2001). Investigation into the deformation of carbon nanotubes and their composites through the use of Raman spectroscopy. Composites Part A: Applied Science and Manufacturing, 32(3-4), 401–411. doi:10.1016/S1359-835X(00)00107-X

Da Silva, A. B., Marini, J., Gelves, G., Sundararaj, U., Gregório, R., & Bretas, R. E. S. (2013). Synergic effect in electrical conductivity using a combination of two fillers in PVDF hybrids composites. European Polymer Journal, 49(10), 3318–3327. doi:10.1016/j.eurpolymj.2013.06.039

Daggumati, S., De Baere, I., Van Paepegem, W., Degrieck, J., Xu, J., Lomov, S. V., & Verpoest, I. (2013). Fatigue and post-fatigue stress–strain analysis of a 5-harness satin weave carbon fibre reinforced composite. Composites Science and Technology, 74, 20–27. doi:10.1016/j.compscitech.2012.09.012

Davis, D. C., Wilkerson, J. W., Zhu, J., & Ayewah, D. O. O. (2010). Improvements in mechanical properties of a carbon fiber epoxy composite using nanotube science and technology. Composite Structures, 92(11), 2653–2662. doi:10.1016/j.compstruct.2010.03.019

Díez-Pascual, A. M., Ashrafi, B., Naffakh, M., González-Domínguez, J. M., Johnston, A., Simard, B., … Gómez-Fatou, M. a. (2011). Influence of carbon nanotubes on the thermal, electrical and mechanical properties of poly(ether ether ketone)/glass fiber laminates. Carbon, 49(8), 2817–2833. doi:10.1016/j.carbon.2011.03.011

Dimchev, M., Caeti, R., & Gupta, N. (2010). Effect of carbon nanofibers on tensile and compressive characteristics of hollow particle filled composites. Materials & Design, 31(3), 1332–1337. doi:10.1016/j.matdes.2009.09.007

Du, J., Wang, S., You, H., & Zhao, X. (2013). Understanding the toxicity of carbon nanotubes in the environment is crucial to the control of nanomaterials in producing and processing and the assessment of health risk for human: A review. Environmental Toxicology and Pharmacology, 36(2), 451–462. doi:10.1016/j.etap.2013.05.007

Green, K. J., Dean, D. R., Vaidya, U. K., & Nyairo, E. (2009). Multiscale fiber reinforced composites based on a carbon nanofiber/epoxy nanophased polymer matrix: Synthesis, mechanical, and thermomechanical behavior. Composites Part A: Applied Science and Manufacturing, 40(9), 1470–1475. doi:10.1016/j.compositesa.2009.05.010

Guadagno, L., De Vivo, B., Di Bartolomeo, a., Lamberti, P., Sorrentino, a., Tucci, V., Vittoria, V. (2011). Effect of functionalization on the thermo-mechanical and electrical behavior of multi-wall carbon nanotube/epoxy composites. Carbon, 49(6), 1919–1930. doi:10.1016/j.carbon.2011.01.017

Hapuarachchi, T. D., & Peijs, T. (2010). Multiwalled carbon nanotubes and sepiolite nanoclays as flame retardants for polylactide and its natural fibre reinforced composites. Composites Part A: Applied Science and Manufacturing, 41(8), 954–963. doi:10.1016/j.compositesa.2010.03.004

Harik, V. M., Klinger, J. R., & Bogetti, T. A. (2002). Low-cycle fatigue of unidirectional composites : Bi-linear S − N curves, 24, 455–462.

Hazarika, A., & Maji, T. K. (2014). Strain sensing behavior and dynamic mechanical properties of carbon nanotubes/nanoclay reinforced wood polymer nanocomposite. Chemical Engineering Journal, 247, 33–41. doi:10.1016/j.cej.2014.02.069

Hegde, R. (2009). Structure and properties of nanoclay reinforced polymer films, fibers and nonwovens. Doctoral Dissertations. Retrieved from http://trace.tennessee.edu/cgi/viewcontent.cgi?article=1069&context=utk_graddiss

Hong, S., Lee, H., & Rhim, J. (n.d.). Effects of clay type and content on mechanical , water barrier and antimicrobial properties of agar-based nanocomposite films.

Huang, W., Li, Z., Chen, X., Tian, P., Lu, J., Zhou, Z., Wang, X. (2014). Pressure-controlled growth of piezoelectric low-dimensional structures in ternary fullerene C60/carbon nanotube/poly (vinylidene fluoride) based hybrid composites. Composites Part B: Engineering, 62, 126–136. doi:10.1016/j.compositesb.2014.02.026

Im, J. S., Lee, S. K., In, S. J., & Lee, Y.-S. (2010). Improved flame retardant properties of epoxy resin by fluorinated MMT/MWCNT additives. Journal of Analytical and Applied Pyrolysis, 89(2), 225–232. doi:10.1016/j.jaap.2010.08.003

Iqbal, K., Khan, S.-U., Munir, A., & Kim, J.-K. (2009). Impact damage resistance of CFRP with nanoclay-filled epoxy matrix. Composites Science and Technology, 69(11-12), 1949–1957. doi:10.1016/j.compscitech.2009.04.016

Jahan, N., Narteh, A., Hosur, M., Rahman, M., & Jeelani, S. (2013). Effect of Carboxyl Functionalized MWCNTs on the Cure Behavior of Epoxy Resin, 2013(April), 40–47.

Jia, X., Liu, B., Huang, L., Hui, D., & Yang, X. (2013). Numerical analysis of synergistic reinforcing effect of silica nanoparticle–MWCNT hybrid on epoxy-based composites. Composites Part B: Engineering, 54, 133–137. doi:10.1016/j.compositesb.2013.04.002

Jumahat, A., Soutis, C., Mahmud, J., & Ahmad, N. (2012). Compressive Properties of Nanoclay/Epoxy Nanocomposites. Procedia Engineering, 41(IRIS), 1607–1613. doi:10.1016/j.proeng.2012.07.357

Khan, S. U., Munir, A., Hussain, R., & Kim, J.-K. (2010). Fatigue damage behaviors of carbon fiber-reinforced epoxy composites containing nanoclay. Composites Science and Technology, 70(14), 2077–2085. doi:10.1016/j.compscitech.2010.08.004

Kim, J., Hu, C., Woo, R., & Sham, M. (2005). Moisture barrier characteristics of organoclay?epoxy nanocomposites. Composites Science and Technology, 65(5), 805–813. doi:10.1016/j.compscitech.2004.10.014

Kostopoulos, V., Baltopoulos, a., Karapappas, P., Vavouliotis, a., & Paipetis, a. (2010). Impact and after-impact properties of carbon fibre reinforced composites enhanced with multi-wall carbon nanotubes. Composites Science and Technology, 70(4), 553–563. doi:10.1016/j.compscitech.2009.11.023

Lam, C., Lau, K., Cheung, H., & Ling, H. (2005). Effect of ultrasound sonication in nanoclay clusters of nanoclay/epoxy composites. Materials Letters, 59(11), 1369–1372. doi:10.1016/j.matlet.2004.12.048

Lam, C.-K., Cheung, H., Lau, K., Zhou, L., Ho, M., & Hui, D. (2005). Cluster size effect in hardness of nanoclay/epoxy composites. Composites Part B: Engineering, 36(3), 263–269. doi:10.1016/j.compositesb.2004.09.006

Lee, J. H., Rhee, K. Y., & Lee, J. H. (2010). Effects of moisture absorption and surface modification using 3-aminopropyltriethoxysilane on the tensile and fracture characteristics of MWCNT/epoxy nanocomposites. Applied Surface Science, 256(24), 7658–7667. doi:10.1016/j.apsusc.2010.06.023

Lee, S. K., Bai, B. C., Im, J. S., In, S. J., & Lee, Y.-S. (2010). Flame retardant epoxy complex produced by addition of montmorillonite and carbon nanotube. Journal of Industrial and Engineering Chemistry, 16(6), 891–895. doi:10.1016/j.jiec.2010.09.014

Liu, L., & Wagner, H. D. (2005). Rubbery and glassy epoxy resins reinforced with carbon nanotubes. Composites Science and Technology, 65(11-12), 1861–1868. doi:10.1016/j.compscitech.2005.04.002

Lu, M., Lau, K., Tam, W.-Y., & Liao, K. (2006). Enhancement of Vicker's hardness of nanoclay-supported nanotube reinforced novel polymer composites. Carbon, 44(2), 383–386. doi:10.1016/j.carbon.2005.09.007

Ma, C. G., Mai, Y. L., Rong, M. Z., Ruan, W. H., & Zhang, M. Q. (2007). Phase structure and mechanical properties of ternary polypropylene/elastomer/nano-CaCO3 composites. Composites Science and Technology, 67(14), 2997–3005. doi:10.1016/j.compscitech.2007.05.022

Manikandan, D., Mangalaraja, R. V., Avila, R. E., Siddheswaran, R., & Ananthakumar, S. (2012). Carbon nanotubes rooted montmorillonite (CNT-MM) reinforced nanocomposite membrane for PEM fuel cells. Materials Science and Engineering: B, 177(8), 614–618. doi:10.1016/j.mseb.2012.02.027

Manjunatha, C. M., Taylor, a. C., Kinloch, a. J., & Sprenger, S. (2010). The tensile fatigue behaviour of a silica nanoparticle-modified glass fibre reinforced epoxy composite. Composites Science and Technology, 70(1), 193–199. doi:10.1016/j.compscitech.2009.10.012

Montazeri, a., & Chitsazzadeh, M. (2014). Effect of sonication parameters on the mechanical properties of multi-walled carbon nanotube/epoxy composites. Materials & Design, 56, 500–508. doi:10.1016/j.matdes.2013.11.013

Morsy, M. S., Alsayed, S. H., & Aqel, M. (2011). Hybrid effect of carbon nanotube and nano-clay on physico-mechanical properties of cement mortar. Construction and Building Materials, 25(1), 145–149. doi:10.1016/j.conbuildmat.2010.06.046

Okada, A., & Usuki, A. (1995). The chemistry of polymer-clay hybrids. Materials Science and Engineering: C, 3(2), 109–115. doi:10.1016/0928-4931(95)00110-7

Olivier, M.-G., Fedel, M., Sciamanna, V., Vandermiers, C., Motte, C., Poelman, M., & Deflorian, F. (2011). Study of the effect of nanoclay incorporation on the rheological properties and corrosion protection by a silane layer. Progress in Organic Coatings, 72(1-2), 15–20. doi:10.1016/j.porgcoat.2010.11.022

Orhan, T., Isitman, N. A., Hacaloglu, J., & Kaynak, C. (2012). Thermal degradation of organophosphorus flame-retardant poly(methyl methacrylate) nanocomposites containing nanoclay and carbon nanotubes. Polymer Degradation and Stability, 97(3), 273–280. doi:10.1016/j.polymdegradstab.2011.12.020

Park, J. G., Cheng, Q., Lu, J., Bao, J., Li, S., Tian, Y., … Wang, B. (2012). Thermal conductivity of MWCNT/epoxy composites: The effects of length, alignment and functionalization. Carbon, 50(6), 2083–2090. doi:10.1016/j.carbon.2011.12.046

Prasad, M. S. S., Venkatesha, C. S., & Jayaraju, T. (2011). Experimental Methods of Determining Fracture Toughness of Fiber Reinforced Polymer Composites under Various Loading Conditions. Journal of Minerals & Materials Characterization & Engineering, 10(13), 1263–1275.

Qian, D., Wagner, G. J., Liu, W. K., Yu, M.-F., & Ruoff, R. S. (2002). Mechanics of carbon nanotubes. Applied Mechanics Reviews, 55(6), 495. doi:10.1115/1.1490129

Rahman, M., Hosur, M., Zainuddin, S., Vaidya, U., Tauhid, A., Kumar, A., Jeelani, S. (2013). Effects of amino-functionalized MWCNTs on ballistic impact performance of E-glass/epoxy composites using a spherical projectile. International Journal of Impact Engineering, 57, 108–118. doi:10.1016/j.ijimpeng.2013.01.011

Rahman, M. M., Zainuddin, S., Hosur, M. V., Malone, J. E., Salam, M. B. a., Kumar, A., & Jeelani, S. (2012). Improvements in mechanical and thermo-mechanical properties of e-glass/epoxy composites using amino functionalized MWCNTs. Composite Structures, 94(8), 2397–2406. doi:10.1016/j.compstruct.2012.03.014

Rahman, M. M., Zainuddin, S., Hosur, M. V., Robertson, C. J., Kumar, a., Trovillion, J., & Jeelani, S. (2013). Effect of NH2-MWCNTs on crosslink density of epoxy matrix and ILSS properties of e-glass/epoxy composites. Composite Structures, 95, 213–221. doi:10.1016/j.compstruct.2012.07.019

Rahmanian, S., Suraya, a. R., Shazed, M. a., Zahari, R., & Zainudin, E. S. (2014). Mechanical Characterization of Epoxy Composite with Multiscale Reinforcements: Carbon Nanotubes and Short Carbon Fibers. Materials & Design. doi:10.1016/j.matdes.2014.03.039

Sahoo, N. G., Rana, S., Cho, J. W., Li, L., & Chan, S. H. (2010). Polymer nanocomposites based on functionalized carbon nanotubes. Progress in Polymer Science, 35(7), 837–867. doi:10.1016/j.progpolymsci.2010.03.002

Salam, M. B. A., Hosur, M. V, Zainuddin, S., & Jeelani, S. (2013). Improvement in Mechanical and Thermo-Mechanical Properties of Epoxy Composite Using Two Different Functionalized Multi-Walled Carbon Nanotubes, 2013. doi:10.4236/ojcm.2013.

Sancaktar, E., & Kuznicki, J. (2011). Nanocomposite adhesives: Mechanical behavior with nanoclay. International Journal of Adhesion and Adhesives, 31(5), 286–300. doi:10.1016/j.ijadhadh.2010.09.006

Sarfaraz, R., Vassilopoulos, A. P., & Keller, T. (2012). A hybrid S–N formulation for fatigue life modeling of composite materials and structures. Composites Part A: Applied Science and Manufacturing, 43(3), 445–453. doi:10.1016/j.compositesa.2011.11.008

Shang, Q. (1999). Mineral Fillers in Thermoplastics I, 139, 1–2. doi:10.1007/3-540-69220-7

Shirkavand Hadavand, B., Mahdavi Javid, K., & Gharagozlou, M. (2013). Mechanical properties of multi-walled carbon nanotube/epoxy polysulfide nanocomposite. Materials & Design, 50, 62–67. doi:10.1016/j.matdes.2013.02.039

Soliman, E. M., Sheyka, M. P., & Taha, M. R. (2012). Low-velocity impact of thin woven carbon fabric composites incorporating multi-walled carbon nanotubes. International Journal of Impact Engineering, 47, 39–47. doi:10.1016/j.ijimpeng.2012.03.002

Srikanth, I., Kumar, S., Kumar, A., Ghosal, P., & Subrahmanyam, C. (2012). Effect of amino functionalized MWCNT on the crosslink density, fracture toughness of epoxy and mechanical properties of carbon–epoxy composites. Composites Part A: Applied Science and Manufacturing, 43(11), 2083–2086. doi:10.1016/j.compositesa.2012.07.005

Tcherbi-Narteh, A., Hosur, M., Triggs, E., & Jeelani, S. (2013). Thermal stability and degradation of diglycidyl ether of bisphenol A epoxy modified with different nanoclays exposed to UV radiation. Polymer Degradation and Stability, 98(3), 759–770. doi:10.1016/j.polymdegradstab.2012.12.013

Tehrani, M., Boroujeni, a. Y., Hartman, T. B., Haugh, T. P., Case, S. W., & Al-Haik, M. S. (2013). Mechanical characterization and impact damage assessment of a woven carbon fiber reinforced carbon nanotube–epoxy composite. Composites Science and Technology, 75, 42–48. doi:10.1016/j.compscitech.2012.12.005

Teng, C.-C., Ma, C.-C. M., Huang, Y.-W., Yuen, S.-M., Weng, C.-C., Chen, C.-H., & Su, S.-F. (2008). Effect of MWCNT content on rheological and dynamic mechanical properties

of multiwalled carbon nanotube/polypropylene composites. Composites Part A: Applied Science and Manufacturing, 39(12), 1869–1875. doi:10.1016/j.compositesa.2008.09.004

Thostenson, E. T., Ren, Z., & Chou, T.-W. (2001). Advances in the science and technology of carbon nanotubes and their composites: a review. Composites Science and Technology, 61(13), 1899–1912. doi:10.1016/S0266-3538(01)00094-X

Vlasveld, D. P. N., Daud, W., Bersee, H. E. N., & Picken, S. J. (2007). Continuous fibre composites with a nanocomposite matrix: Improvement of flexural and compressive strength at elevated temperatures. Composites Part A: Applied Science and Manufacturing, 38(3), 730–738. doi:10.1016/j.compositesa.2006.09.010

Xu, Y., & Hoa, S. Van. (2008). Mechanical properties of carbon fiber reinforced epoxy/clay nanocomposites. Composites Science and Technology, 68(3-4), 854–861. doi:10.1016/j.compscitech.2007.08.013

Yang, H., Zhang, Q., Guo, M., Wang, C., Du, R., & Fu, Q. (2006). Study on the phase structures and toughening mechanism in PP/EPDM/SiO2 ternary composites. Polymer, 47(6), 2106–2115. doi:10.1016/j.polymer.2006.01.076

Yang, K., Gu, M., Guo, Y., Pan, X., & Mu, G. (2009). Effects of carbon nanotube functionalization on the mechanical and thermal properties of epoxy composites. Carbon, 47(7), 1723–1737. doi:10.1016/j.carbon.2009.02.029

Yang, S.-Y., Lin, W.-N., Huang, Y.-L., Tien, H.-W., Wang, J.-Y., Ma, C.-C. M., Wang, Y.-S. (2011). Synergetic effects of graphene platelets and carbon nanotubes on the mechanical and thermal properties of epoxy composites. Carbon, 49(3), 793–803. doi:10.1016/j.carbon.2010.10.014

Yasmin, a., Luo, J. J., Abot, J. L., & Daniel, I. M. (2006). Mechanical and thermal behavior of clay/epoxy nanocomposites. Composites Science and Technology, 66(14), 2415–2422. doi:10.1016/j.compscitech.2006.03.011

Ye, Y., Chen, H., Wu, J., & Chan, C. M. (2011). Evaluation on the thermal and mechanical properties of HNT-toughened epoxy/carbon fibre composites. Composites Part B: Engineering, 42(8), 2145–2150. doi:10.1016/j.compositesb.2011.05.010

Zainuddin, S., Fahim, a., Arifin, T., Hosur, M. V., Rahman, M. M., Tyson, J. D., & Jeelani, S. (2014). Optimization of mechanical and thermo-mechanical properties of epoxy and E-glass/epoxy composites using NH2-MWCNTs, acetone solvent and combined dispersion methods. Composite Structures, 110, 39–50. doi:10.1016/j.compstruct.2013.11.010

Zainuddin, S., Hosur, M. V., Zhou, Y., Kumar, A., & Jeelani, S. (2009). Durability studies of montmorillonite clay filled epoxy composites under different environmental conditions. Materials Science and Engineering: A, 507(1-2), 117–123. doi:10.1016/j.msea.2008.11.058

Zainuddin, S., Hosur, M. V., Zhou, Y., Narteh, A. T., Kumar, A., & Jeelani, S. (2010). Experimental and numerical investigations on flexural and thermal properties of nanoclay–epoxy nanocomposites. Materials Science and Engineering: A, 527(29-30), 7920–7926. doi:10.1016/j.msea.2010.08.078

Zhou, Y., Akanda, S. R., Jeelani, S., & Lacy, T. E. (2007). Nonlinear constitutive equation for vapor-grown carbon nanofiber-reinforced SC-15 epoxy at different strain rate. Materials Science and Engineering: A, 465(1-2), 238–246. doi:10.1016/j.msea.2007.04.042

Zhou, Y., Pervin, F., Jeelani, S., & Mallick, P. K. (2008). Improvement in mechanical properties of carbon fabric–epoxy composite using carbon nanofibers. Journal of Materials Processing Technology, 198(1-3), 445–453. doi:10.1016/j.jmatprotec.2007.07.028

Zhou, Y., Pervin, F., Rangari, V. K., & Jeelani, S. (2007). Influence of montmorillonite clay on the thermal and mechanical properties of conventional carbon fiber reinforced composites. Journal of Materials Processing Technology, 191(1-3), 347–351. doi:10.1016/j.jmatprotec.2007.03.059